PART TWO

SELECTIVE OXIDATION OF ETHANE VIA HETEROPOLYANION-CONTAINING SOLID CATALYSTS

CHAPTER SEVEN

SELECTIVE OXIDATION OF LIGHT ALKANES

7.1 Introduction

Oxidation steps are critical to the functionalization of chemicals and intermediates. Over 60% of chemicals and intermediates are prepared via a catalytic oxidation step at some stage of their production.[1] Many fine chemical processes use stoichiometric oxidants, e.g., permanganates and chromium salts that are harmful to the environment. Catalytic processes are attractive because they reduce the consumption of environmentally harmful oxidants and can improve the economics of the oxidation process. In the development of catalytic materials, often molecular oxygen (O_2) or hydrogen peroxide (H_2O_2) can be used. This enables the process to be more environmentally friendly, because water is the co-product of reaction. Catalytic oxidations suffer from substrate-specificity, i.e., a particular catalyst is only effective for one reactant/product or set of reaction conditions. The versatility of many oxidation catalysts is limited, thereby restricting their industrial usefulness.

Some catalytic oxidation processes are listed in Table 7.1. The catalysts for these processes have been optimized for a particular reaction and set of conditions. The production of vinyl acetate results from a two-step oxidation. First the acetic acid is produced from carbonylation of methanol. The acetic acid is then reacted with ethylene in the presence of air to make vinyl acetate. Some of the reactants, e.g., methanol and propylene, are already partially oxidized. Typically, alkenes and aromatics are used as feedstocks because they are easy to functionalize. Alkenes are becoming particularly costly, as the demand for high purity alkenes as raw materials for many industrial processes (such as monomers or comonomers in polymerization) increases. It is desirable to remove the need for alkene feedstocks in the preparation of chemical

intermediates wherever feasible. The use of light alkanes as reactants for selective oxidation would allow one to take advantage of an under-utilized and relatively inexpensive feedstock and avoid competition with other processes for alkene raw materials. Currently, the selective oxidation of *n*-butane to maleic anhydride is the only catalytic commercial oxidation process that uses a light alkane as a reactant. Other light alkanes, i.e., methane, ethane and propane, are of interest as possible routes to methanol and formaldehyde (methane), acetic acid (ethane), and acrylic acid or acrylonitrile (propane).[1] The current production methods for these intermediates consist of multiple step processes through partially oxygenated raw materials which themselves must be produced (see Table 7.2).

The challenge of alkane use is that alkanes are more difficult to activate than alkenes. Alkane dehydrogenations to the corresponding alkene are typically performed at high temperatures (500-800^{o}C) and are thermodynamically limited in the yield of alkenes.[2] Dehydrogenation catalysts also have a tendency to deactivate due to coking or thermal instability. Ethane dehydrogenation must be performed at particularly high temperatures in order to activate the C-H bond. Oxidative dehydrogenation is more thermodynamically favorable and allows the alkenes to be formed at lower temperatures (300-400^{o}C), with less catalyst deactivation and coking. With the addition of oxygen into the reaction, however, alkane combustion becomes possible and allows over-oxidation products to form. Combustion products CO and CO_2 (referred to as total oxidation products, CO_x) are favored thermodynamically. The use of propane and butane for selective oxidation is difficult because both the alkenes and the liquid oxygenates are particularly susceptible to additional oxidation to CO_x. The high reaction temperatures

required to allow effective alkane activation increase the tendency of the oxygenated products to undergo total oxidation. Ethylene, rather than acetic acid, is usually the preferred product of ethane oxidation.[3] Selectivity control, forming the desired oxygenated product easily yet avoiding over-oxidation, becomes important for new catalyst development. A variety of catalyst systems have been studied for alkane activation: mixed metal oxides (bulk[4-7] or supported[8,9]), heteropolyacids, [10-14] and molecular sieves.[15-19] However, these catalyst systems are limited in versatility and robustness and are usually specific to a particular alkane substrate. An ideal selective oxidation catalyst would be able to activate light alkanes and be versatile for multiple substrates and products of reaction.

7.2 Ethane Selective Oxidation Catalysts

An effective catalyst for the selective oxidation of ethane was reported by Thorsteinson and co-workers.[20] The catalyst, a V/Nb/Mo oxide mixture optimized to composition of $Mo_{0.73}V_{0.18}Nb_{0.09}O_x$, was very active for the oxidative dehydrogenation to ethylene, even at temperatures as low as 200^{o}C. Appreciable formation of ethylene was observed at atmospheric pressure and 350^{o}C with 58% ethane conversion and 65% selectivity (see Table 7.3). No acetic acid was observed at atmospheric pressure. Ruth *et al*. reported the formation of acetic acid (2.5% selectivity) with the Thorsteinson catalyst at elevated pressures (290 psig).[21] At these conditions, a STY of 0.022 mmol/min/g catalyst of acetic acid could be produced. However, this catalyst was a complex mixture of different oxide phases that was difficult to prepare. Several studies found that differences in oxide preparation affected the catalyst performance.[1]

The use of promoters has been studied to modify the activity and selectivity of the V/Nb/Mo oxide Thorsteinson catalyst. The addition of a small amount of Pd to the mixed oxide ($Mo_1V_{0.25}Nb_{0.12}Pd_{0.0005}O_x$) improved the selectivity to acetic acid (see Table 7.3).[22] Linke and co-workers also reported that the partial pressure of steam fed affected the catalyst performance. Other systems, such as vanadium oxides supported on titania, have bee studied. Yet in the literature, acetic acid yields have generally remained low and often can only be obtained at elevated pressure.

7.3 Heteropolyanions

Heteropolyanions (HPAs) are polyoxometalates with one or more central organizing polyhedrons (the central atom being referred to as the "heteroatom," e.g., Si^{4+}, Ge^{4+}, P^{5+}, or As^{5+}) about which "addenda" metal-oxygen polyhedrons (e.g., Mo^{6+} or W^{6+}) are arranged. The addenda metals can have other metal substitution (e.g., V or Nb). These metal oxide clusters have the general formula $[X_xM_mO_y]^{q-}$, where X is the heteroatom and M is the addenda atom. They are prepared by self-assembly in aqueous solutions and can be synthesized in a variety of structures and compositions (e.g., the Keggin unit, where $x = 1$, $m = 12$, and $y = 40$).[23] The overall anionic charge of the compound may be countered with protons or other cations (organic and inorganic) to make the corresponding salt.

These materials, unlike zeolites and other bulk metal oxides that have metal-oxygen lattices, consist of discrete anionic units of metal oxide that are the primary structure of the material. The primary structures are associated by the interstitial guest species (e.g., water) to arrange in a uniform fashion into crystals to form a secondary structure. Organic guest species (e.g., alcohols, ethers, amines) may also be incorporated

into the interstitial spaces between the metal oxide clusters. Aggregates of the secondary structures form a tertiary structure that describes the physical characteristics of the material (e.g., porosity, particle size, and surface area). Variations in the structure and composition affect the acidic and oxidative nature of these HPAs and thereby affect their activity and selectivity in oxidation reactions. Many reviews have documented the catalytic uses of HPAs, especially in homogeneous reactions at moderate temperatures (see Refs. 14 and 23 and citations therein.) Thermal decomposition of the *acid* form of HPAs has limited the application of these compounds as gas phase oxidation catalysts. The acid HPAs decompose from 200-400^{o}C, depending on the composition, into a mixture of metal oxides.

Heteropolyanion salts, which are more stable, have been shown to be useful in gas phase oxidation reactions (see Table 7.4). HPAs have been used in the oxidation of a variety of substrates, including alkanes, alkenes, and alcohols. Sb and W-containing HPAs have been used for the oxidation of ethane to ethylene at elevated temperatures.[10] Showa Denko demonstrated that ethylene can be oxidized to acetic acid using Pd-$H_4[SiW_{12}O_{40}]$[24]. No formation of acetic acid was observed with either Pd(0) alone or HPA alone on silica. This method of acetic acid production is superior to the traditional methanol carbonylation because it eliminates the need for high purity CO as a feedstock and the use of expensive materials of construction. Mizuno and co-workers reported the use of Cs-containing HPAs, combined with another metal (depending on reaction), for the oxidation of alkanes (see Table 7.5).[14,23] Ethane and propane were both oxidized to their alkenes. Formic acid, acrylic acid, and methacrylic acid were formed from methane, propane, and isobutane, respectively.

Ueda and co-workers reported that a pyridine-exchanged heteropolyanion, pretreated to 420^{o}C under flowing inert, was used as a precursor to a catalyst for the oxidation of light alkanes. The active phase formed from the HPA precursor was active for propane oxidation, having 12% conversion and 24% selectivity to acrylic acid.[11,13] This catalyst system was later shown to also convert ethane to acetic acid at 340^{o}C with 10% selectivity at 1% ethane conversion.[11]

7.4 Objectives

Previous work by Davis and co-workers[25-28] reported the development of a versatile selective oxidation catalyst system using HPA salts as catalyst precursors that was highly active and selective for both the oxidation of *n*-butane to maleic acid and the oxidation of propane to acrylic acid. The catalysts were formed from niobium- and pyridine-exchanged HPAs, specifically molybdophosphoric acid ($H_3PMo_{12}O_{40}$) and molybdovanadophosphoric acid ($H_4PMo_{11}VO_{40}$), by heat treatment to 420^{o}C under helium. The catalysts are active over a range of reaction temperatures and with either hydrocarbon-rich or oxygen-rich flows. The focus of this project is to explore whether the new HPA catalyst system developed by Davis and co-workers could be used for the selective oxidation of ethane to acetic acid and ethylene.

7.5 References

(1) Centi, G. *et al., Selective Oxidation by Heterogeneous Catalysis*; Kluwer Academic/Plenum Publishers: New York, 2001.

(2) Bhasin, M. M. *Top. Catal.* **2003**, *23*, 145.

(3) Cavani, F.; Trifiro, F. *Catal. Today* **1999**, *51*, 561.

(4) Novakova, E. K. *et al., J. Catal.* **2002**, *211*, 226.

(5) Solsona, B. *et al., Appl. Catal., A* **2003**, *249*, 81.

(6) Grasselli, R. K. *et al., Top. Catal.* **2003**, *23*, 5.

(7) Ledoux, M. J. *et al., J. Catal.* **2001**, *203*, 495.

(8) Solsona, B. *et al., J. Catal.* **2001**, *203*, 443.

(9) Kucherov, A. V. *et al., Catal. Today* **2003**, *81*, 297.

(10) Cavani, F. *et al., Catal. Today* **1995**, *24*, 365.

(11) Li, W.; Ueda, W. *Stud. Surf. Sci. Catal.* **1997**, *110*, 433.

(12) Li, W. *et al., Appl. Catal., A* **1999**, *182*, 357.

(13) Ueda, W.; Suzuki, Y. *Chem. Lett.* **1995**, *7*, 541.

(14) Mizuno, N.; Misono, M. *Chem. Rev.* **1998**, *98*, 199.

(15) Luo, L. *et al., J. Catal.* **2001**, *200*, 222.

(16) Marchese, L. *et al., J. Catal.* **2002**, *208*, 479.

(17) Bulanek, R. *et al., Appl. Catal., A* **2002**, *235*, 181.

(18) Zhang, Q. *et al., J. Catal.* **2001**, *202*, 308.

(19) Concepcion, P. *et al., Microporous Mesoporous Mater.* **2004**, *67*, 215.

(20) Thorsteinson, E. M. *et al., J. Catal.* **1978**, *52*, 116.

(21) Ruth, K. *et al., J. Catal.* **1998**, *175*, 27.

(22) Linke, D. *et al., J. Catal.* **2002**, *205*, 16.

(23) Kozhevnikov, I. V. *Catalysis by Polyoxometalates*; John Wiley & Sons, 2002.

(24) Suzuki, T. *et al.,* ; Showa Denko Kabushiki Kaisha: European, 1994.

(25) Davis, M. E. *et al., Angew. Chem., Int. Ed.* **2002**, *41*, 858.

(26) Holles, J. H. *et al., J. Catal.* **2003**, *218*, 42.

(27) Dillon, C. J. *et al., J. Catal.* **2003**, *218*, 54.

(28) Dillon, C. J. *et al., Catal. Today* **2003**, *81*, 189.

(29) Tessier, L. *et al., Catal. Today* **1995**, 335.

Table 7.1 Current commercial production of chemical intermediates. Adapted from ref. 1.

Reactants	Products	Conversion (%)	Selectivity (%)
Methanol/ Air	Formaldehyde	99	94
Propylene/ Air/ Ammonia	Acrylonitrile	97-99	73-82
Methanol/ CO (30 bar)	Acetic Acid	-	99
Ethylene/ Acetic Acid/ Air	Vinyl Acetate	20-35	98-99
n-Butane/ Air	Maleic Anhydride	70-80	65-70

Table 7.2 Alkane oxidations of development interest. Adapted from ref. 1.

Product	Possible Alkane Source	Current Technology
Methanol	Methane	Two-Step Methane Steam Reforming
Formaldehyde	Methane	Three-Step Methanol Oxidation
Acetic Acid	Ethane	Multi-Step Methanol Carbonylation
Acrylic Acid	Propane	Two-Step Process through Acrolein
Acrylonitrile	Propane	Propylene Ammoxidation

Table 7.3 Selective ethane oxidation catalysts.

Catalyst	T	P	Flow	Conv.	Selectivity		STY[b]		Ref.
	(C)	(psig)	C_2: O_2: I[a]: H_2O	(%)	$C_2^=$	Ac	$C_2^=$	Ac	
$Mo_{0.73}V_{0.18}Nb_{0.09}O_x$	350	0	13.3: 8.8: 125: 0	58	65	0	0.007	0	20
	350	290	6: 3.6: 14.4: 0	32	44	2.5	0.39	0.022	21
$Mo_1V_{0.25}Nb_{0.12}Pd_{0.0005}O_x$	246	218	7.3: 1.5: 9.5: 0.1	4.7	1	59	0.004	0.012	22
VO_x/TiO_2	250	0	142: 8.3: 16.7: 0	1	18	36	0.004	0.007	29

[a]I = inert (He, N_2)

[b]STY is in mmol/min/g catalyst

Table 7.4 Gas-phase oxidations with heteropolyanion catalysts. Adapted from ref. 23.

Reaction	Catalyst	T (C)
Methacrolein + O_2 → Methacrylic Acid	$CsH_3[PMo_{11}VO_{40}]$	260
Isobutane + O_2 → Methacrylic Acid	$H_3[PMo_{12}O_{40}]$	350
n-Butane + O_2 → Maleic Anhydride	$Bi[PMo_{12}O_x] + VO^{2+}$	360
$CH_4 + N_2O$ → HCHO, CH_3OH	$H_3[PMo_{12}O_{40}]/SiO_2$	570
$CH_3OH + O_2$ → HCHO, $(CH_3)_2O$	$H_3[PMo_{12}O_{40}]$	200-290
$C_2H_5OH + O_2$ → CH_3CHO, $(C_2H_5)_2O$	$H_3[PMo_{12}O_{40}]$ + polysulfone	170
Isobutene + O_2 → Methacrolein	$PbFeBi[PMo_{12}O_x]$	400

Table 7.5 Selective oxidation of light alkanes with HPAs. Adapted from ref. 14.

Reaction	Catalyst	T (C)	Yield (%)
Methane → Formic Acid	$Cs_{2.5}Pd_{0.08}H_{1.34}[PVMo_{11}O_{40}]$	300	0.05
Ethane → Ethylene	$Cs_{2.5}Mn_{0.08}H_{1.34}[PVMo_{11}O_{40}]$	425	4.3
Propane → Acrylic Acid	$Cs_{2.5}Fe_{0.08}H_{1.26}[PVMo_{11}O_{40}]$	380	13
Propane → Propylene	$Cs_{2.5}Cu_{0.08}H_{3.34}[PV_3Mo_9O_{40}]$	380	10
Isobutane → Methacrylic Acid	$Cs_{2.5}Ni_{0.08}H_{1.26}[PVMo_{11}O_{40}]$	340	9.0

CHAPTER EIGHT

REACTIVITY OF NIOBIUM- AND PYRIDINE-EXCHANGED HETEROPOLYANIONS FOR THE CONVERSION OF ETHANE

8.1 Introduction

Holles *et al*. described the preparation and alkane oxidation reactivity of niobium and pyridine-containing phosphomolybdates.[1] Specifically, molybdophosphoric acid ($H_3PMo_{12}O_{40}$, denoted PMo_{12}) and molybdovanadophosphoric acid ($H_4PMo_{11}VO_{40}$, denoted $PMo_{11}V$) were exchanged with niobium oxalate and pyridine to produce the exchanged HPAs (denoted $NbPMo_{12}$pyr and $NbPMo_{11}V$pyr, respectively). The active catalyst was obtained by pretreatment of the exchanged HPAs in flowing helium to 420^{o}C.

The catalysts were thoroughly characterized by TGA/DSC, ^{31}P MAS NMR, and *in situ* XRD, XAS, and XPS, described by Dillon *et al*.[2] XRD and ^{31}P MAS NMR showed that the Keggin unit remained intact during the niobium and pyridine exchange process. *In situ* XRD showed that without pyridine exchanged into the HPA, the Keggin unit decomposed to MoO_3 at elevated temperatures (>500^{o}C). In samples containing both niobium and pyridine, the Keggin unit decomposed to MoO_2 at elevated temperatures (>500^{o}C). Neither MoO_3 nor MoO_2 were active for selective oxidation. However, a mostly amorphous phase formed at 420^{o}C in samples containing both niobium and pyridine. This phase was found to be active for selective oxidation of light alkanes. Thermagravimetric analysis and elemental analysis showed that by 420^{o}C, all of the pyridine was removed from the material. During removal of pyridine by heat treatment to 420^{o}C, the Keggin structure decomposed to lacunary structures, as seen by ^{31}P MAS NMR. The catalyst was found to be in a reduced oxidation state after heat treatment, where Nb^{5+} was reduced to Nb^{4+} and some of the Mo^{6+} was reduced to Mo^{5+}.

These catalysts were shown to be active for *n*-butane oxidation (see Table 8.1). [1] Butane reactivity was tested at flow rates of 4: 2: 4: 5 mL/min of butane: oxygen: helium: steam and 380^{o}C (using 0.2 g of $NbPMo_{12}pyr$). The incorporation of pyridine was shown to be essential for active catalyst formation; PMo_{12} and $PMo_{11}V$ had no significant conversion under the same conditions. The niobium-exchanged materials, without pyridine, (denoted $NbPMo_{12}$, and $NbPMo_{11}V$, respectively) also showed no activity. The pyridine-exchanged materials (denoted $PMo_{12}pyr$ and $PMo_{11}Vpyr$, respectively) each had high activity, with butane conversions of 13.5%. Maleic acid selectivity (formed from maleic anhydride as liquid oxygenates were trapped in water for analysis) was also high (82 and 90% for $PMo_{12}pyr$ and $PMo_{11}Vpyr$, respectively).

The incorporation of both niobium and pyridine resulted in active catalysts as well. $NbPMo_{12}pyr$ gave 15% conversion of butane, utilizing all of the oxygen available (15% was the maximum theoretical conversion at the butane: oxygen ratio of 2:1). Maleic acid was the major product, having 71% selectivity. 25% selectivity to total oxidation product (CO_x) was observed, with small amounts of acetic acid and acrylic acid also being formed. $NbPMo_{11}Vpyr$ also had high butane conversion (15%) and selectivity to maleic acid (76%).

Although the addition of only pyridine to the HPA precursor resulted in active catalysts at lower flow rates, only 2.5% butane conversion was observed after an eight-fold increase in flow rates (32: 16: 32: 40 mL/min) with $PMo_{12}pyr$. The addition of both niobium and pyridine was essential for catalyst activity at higher flow rates. $NbPMo_{12}pyr$ gave a butane conversion of 15% and maleic acid selectivity of 90% at the higher flow rates. This resulted in a space time yield (STY) of maleic acid of 0.84 mmol/min/g

catalyst. Similar results were obtained with $NbPMo_{11}Vpyr$, having 14% butane conversion and 80% selectivity to maleic acid at 380°C and flow rates to 32: 16: 32: 40 mL/min of butane: oxygen: helium: steam, giving a STY of 0.76 mmol/min/g catalyst of maleic acid.

The same catalysts were also examined in the oxidation of propane to acrylic acid (see Table 8.2). As in the butane oxidation, neither of the acid forms of the HPAs (PMo_{12} and $PMo_{11}V$) had activity for propane oxidation (0.4% conversion for $PMo_{11}V$, at 380°C and flow rates of 8: 4: 8: 10 mL/min of propane: oxygen: helium: steam). The addition of Nb did not significantly affect activity for propane with $NbPMo_{11}V$ (1.4% conversion). Unlike the butane studies, even the addition of pyridine to make $PMo_{11}Vpyr$ did not yield an active propane oxidation catalyst (3.4% conversion).

The addition of both niobium and pyridine was necessary for an active catalyst at these conditions (25% conversion for both $NbPMo_{12}pyr$ and $NbPMo_{11}Vpyr$). However, $NbPMo_{12}pyr$ resulted in a significant amount of CO_x (79% selectivity) with little acrylic acid (2%). Some maleic acid and acetic acid was also observed (14% and 2%, respectively). The substitution of vanadium into the HPA framework prevented over-oxidation to CO_x. At the same conditions and conversion, $NbPMo_{11}Vpyr$ had only 15% selectivity to CO_x and 21% to acrylic acid. Maleic acid and acetic acid selectivities were 43% and 19%, respectively. The product distribution between acrylic acid and maleic acid was affected by space velocity. Acrylic acid selectivity was increased to 49% (from 21%) and maleic acid decreased to 15% (from 43%) by the increase of flows of 32: 16: 32: 40 mL/min at 380°C (with 21% propane conversion). Acetic acid selectivity remained similar at 23%.

Preliminary work in these studies indicated that the exchanged HPAs would also be effective for the oxidation of ethane to acetic acid.[1] The catalytic study of the ethane oxidation was examined here to determine optimal process conditions, e.g., reaction temperature, pressure, flow composition, and HPA composition.

8.2 Experimental Section

8.2.1 $NbPMo_{12}pyr$ Preparation

Niobium pentachloride ($NbCl_5$) was purchased from Aldrich and stored in a desiccator. The $NbCl_5$ (1.867 g) was dissolved in 15.0 mL of water. The water was added drop wise via pipet to the solid with vigorous stirring. The mixture was stirred at room temperature until a clear solution resulted. Ammonium hydroxide (3.0 mL) was added to basify the solution (pH = 12), and its addition produced a white precipitate, presumed to be niobium oxide. The precipitate was recovered by filtration and washing with ammonium hydroxide. The resulting white paste was allowed to dry exposed to ambient air overnight. Oxalic acid (1.560 g, purchased from Aldrich) was dissolved in 30 mL of water. The oxalic acid solution was then added drop wise via pipet to the dried niobium oxide with vigorous stirring. The slurry was stirred and heated to 80^{o}C for 1-2 hours to allow the niobium oxide to completely dissolve. The resulting clear niobium oxalate solution was then allowed to cool to room temperature.

Molybdophosphoric acid, $H_3PMo_{12}O_{40}$ (hereafter denoted PMo_{12}) was purchased from Aldrich. PMo_{12} (yellow solid, 30.097 g) was dissolved in 46 mL of water to produce a clear, yellow solution. The niobium oxalate solution was added drop wise with stirring to the PMo_{12} solution. The Nb-exchanged PMo_{12} material, hereafter denoted $NbPMo_{12}$, was allowed to heat to dryness, exposed to ambient air, overnight at 80^{o}C to

produce green solids. The $NbPMo_{12}$ (21.235 g) was crushed to a fine powder and dissolved in 127 mL of water. A solution of pyridine (6.650 g) and water (68 mL) was added slowly drop wise to the $NbPMo_{12}$ solution. A light green precipitate began to form as pyridine was added. The pyridine-exchanged $NbPMo_{12}$, hereafter denoted $NbPMo_{12}$pyr, was heated to dryness exposed to ambient air overnight at 80°C to produce light green solids. Samples of $NbPMo_{12}$pyr were prepared having Nb/Keggin loadings of 0.04, 0.2, 0.4 (recipe shown), 0.6, 0.8, and 1.0 (see Figure 8.1). Samples were also prepared having only Nb-exchange (no pyridine) and pyridine alone (see Figure 8.2). It is important to note that unless otherwise stated, all $NbPMo_{12}$pyr results are given for a Nb/Keggin ratio of 0.4.

8.2.2 $NbPMo_{11}V$pyr Preparation

Molybdovanadophosphoric acid, $H_4PMo_{11}VO_{40}$ (denoted $PMo_{11}V$), was prepared according to known methods,[3] by Holles and co-workers.[1] The Nb- and pyridine-exchange was then preformed as described above to prepare $NbPMo_{11}V$pyr (see Figure 8.3). Samples of $NbPMo_{11}V$pyr prepared by Holles and co-workers have a Nb/Keggin loading of 0.04, 0.12, 0.68, 0.87, and 0.98 (see Figure 8.4). It is important to note that unless otherwise stated, all $NbPMo_{11}V$pyr results are given for a Nb/Keggin ratio of 0.68.

Alternatively, $PMo_{11}V$ was purchased from Pred Materials, and ammonium niobium oxalate was obtained from HC Stark. Using these commercially available sources, $NbPMo_{11}V$pyr was also prepared. Ammonium niobium oxalate (0.508 g) was dissolved in 4.5 mL of water. The slurry was heated to 80°C for 2 to 4 hours and allowed to stir covered at room temperature for 48 hours until only slightly cloudy. $PMo_{11}V$ (orange solid, 3.862 g) was dissolved in 6 mL of water to produce a clear, orange

solution. The niobium oxalate solution was added drop wise to the $PMo_{11}V$ solution. The Nb-exchanged $PMo_{11}V$ material, denoted $NbPMo_{11}V$, was heated to dryness overnight at 80°C to produce dark green solids. The $NbPMo_{11}V$ (2.835 g) was crushed to a fine powder and dissolved in 17 mL of water. A solution of pyridine (0.915 g) and water (9 mL) was added slowly drop wise to the $NbPMo_{11}V$ solution. A light green precipitate began to form as pyridine was added. The pyridine-exchanged $NbPMo_{11}V$, hereafter denoted $NbPMo_{11}Vpyr$, was heated to dryness, exposed to ambient air, overnight at 80°C to produce orange-green solids. The sample of $NbPMo_{11}Vpyr$ prepared with ammonium niobium oxalate has a Nb/Keggin loading of 0.68.

8.2.3 Reactivity Studies

Ethane reactions were performed in two BTRS Jr. Reactors (Autoclave Engineers, see Figure 8.5 for reactor schematics and Appendix A for reactor photos), each equipped with a ½-inch stainless steel reactor tube. One reactor was equipped with a back pressure regulator (purchased from Tescom Corp., special order model # 44-2300) and capable of reaction at high pressures (referred to hereafter as "high pressure reactor"). The second reactor was only equipped to run at atmospheric pressure (referred to hereafter as "low pressure reactor"). It is important to note that mixtures of alkanes and oxygen may be flammable at certain compositions. Caution was taken to ensure that the gas feed compositions used in the reactions were non-flammable. A detailed discussion of the flammability range calculations for ethane is presented in Appendix B. Feed gases consisted of ethane (99.99%, Matheson), oxygen (99.5%, Air Liquide), and 5% argon in helium (99.999%, Air Liquide). Ethylene (99.5%, Matheson) was also used to replace ethane to probe the mechanism of acetic acid formation. For pressurized reactions, the

feed rates were 8: 4: 27: 10 mL/min of ethane: oxygen: helium: steam. Atmospheric reactions had feed flow rates of 16: 8: 16: 20 mL/min of the same gases.

A standard catalyst volume of 0.6 mL was used, giving a gas hourly space velocity (GHSV) of 4500 hr^{-1} for pressurized experiments and 6000 hr^{-1} for atmospheric experiments. The catalyst (35-60 mesh) was dispersed in 1 mL of silicon carbide (16 mesh, purchased from Abrasives Unlimited), held in place by glass wool. The catalyst was pretreated *in situ* under flowing helium (200 mL/min) to 420^{o}C, at a heating rate of 1.3^{o}/min, and held for 10 hours. Gas streams were controlled by mass flow controller systems (purchased from Brooks Instruments). Liquid water was fed by syringe pump into the reactant gas mixing area, which was heated to allow complete vaporization (150-170^{o}C for reaction at atmospheric pressure, 235^{o}C for reaction at 230 psig).

The reactor effluent was fed directly to a multi-port valve for gas sampling. The product lines from the reactor and the sample valve were heated to approximately 150^{o}C to prevent liquid condensation. The product analysis was done by GC/MS (HP 6890N), having a capillary column (HP Plot Q). Samples were run at a temperature program of 120^{o}C for two minutes (to allow gas sampling) and then heating to 250^{o}C at 10^{o}/min. A known amount of argon in the helium feed stream to the reactor (see above) was used for an internal standard.

8.3 Results and Discussion

8.3.1 Study of $Nb_{0.4}PMo_{12}$pyr in High Pressure Ethane Reactions

The behavior of the ethane oxidation for $NbPMo_{12}$pyr was studied under pressure, at 230 psig, having flow rates of 8: 4: 27: *x* mL/min ethane: oxygen: helium: steam, where *x* was varied from 0 to 10. At a 2:1 ethane/oxygen ratio, the maximum theoretical

conversion of ethane, assuming total selectivity to ethylene (requiring the least amount of oxygen) is 33%. With no steam added to the feed stream, ethane conversion was 15.0% (see Figure 8.6). Selectivity was mostly to CO_x (83.4%). Some ethylene ($C_2^=$) was formed (12.7%), and some acetic acid (Ac) was formed (3.9%). As steam was introduced to the feed, the conversion decreased. With decreasing conversion, selectivity to ethylene and acetic acid improved. At the highest steam feed observed (10 mL/min), the ethane conversion had dropped to 6.0%, but the ethylene and acetic acid selectivities had increased to 23.2% and 12.4%, respectively. The balance of the products formed was CO_x (64.5%).

As seen from the data given in Figure 8.7, however, the changes in conversion and selectivity do not affect the space time yield (STY) of acetic acid formed (0.003 mmol acetic acid/ min/ g catalyst for both $x = 0$ and 10 mL/min). A plot of product selectivity vs. conversion (see Figure 8.8) showed the relationship between conversion and selectivity. As conversion increased, preference for selective oxidation products (ethylene and acetic acid) decreased and total oxidation products (CO_x) increased. These result indicate that the variation of steam fed does not alter the reactivity of the system, and the changes observed in selectivity were simply a function of changes in the conversion. The amount of steam fed thus could not be used to significantly change the acetic acid production, and there was no optimal steam feed rate observed.

The effect of reaction temperature was examined at 230 psig and flows of 8: 4: 27: 10 mL/min of ethane: oxygen: helium: steam. As seen in the data given in Table 8.3, increasing temperature increased the ethane conversion, from 0.4% at 240^{o}C to 8.1% at 330^{o}C. Note that the homogeneous gas phase oxidation of ethane becomes dominant

upon further increase in temperature (T > 350^{o}C at 230 psig). As the conversion increased, the selectivity to CO_x also increased from 18.3% to 59.5% as the temperature was increased from 240 to 330^{o}C, respectively. The selectivity to ethylene and acetic acid was high at 240^{o}C (59.1 and 22.6%, respectively), but dropped to 35.7 and 4.8%, respectively, at 330^{o}C. The highest STY of ethylene produced was 0.015 mmol/min/g catalyst at 330^{o}C. The highest STY of acetic acid produced was 0.003 mmol/min/g catalyst at 280^{o}C.

The GHSV was decreased, by increasing catalyst amount up to 2.4 mL in 2 grams of silicon carbide, over several runs for ethane reaction at 280^{o}C, 230 psig, and flows of 8: 4: 27: 10 mL/min ethane: oxygen: helium: steam. In general, decreasing the space velocity increased the ethane conversion, but mostly CO_x was produced (see Figure 8.9). Acetic acid and ethylene selectivity decreased as GHSV decreased. Over-oxidation to CO_x occurred due to longer residence times in the catalyst bed at lower space velocities. Thus, decreasing the space velocity from 4500 to 1200 hr^{-1} dropped the ethylene STY from 0.006 to 0.002 mmol/min/g catalyst (see Figure 8.10). A similar decrease in acetic acid production, from 0.003 to $4.9x10^{-4}$ mmol/min/g catalyst was observed. At similar GHSV, except with no steam fed, the competition between conversion and selectivity was again observed (see Table 8.4). By decreasing the space velocity, total oxygen consumption was observed, but primarily to CO_x (~90%). No significant changes in the production of acetic acid could be made by space velocity adjustments.

Holles *et al*. reported that Nb- and pyridine-exchange was critical for the HPA precursor to be an active catalyst for propane oxidation and for activity at high space velocities in the butane system.[1] In order to test the ethane system for similar results,

samples of PMo_{12}, $NbPMo_{12}$, and PMo_{12}pyr were used as catalyst precursors for reaction at 280°C, 230 psig, and flows of 8: 4: 27: 10 mL/min ethane: oxygen: helium: steam (see Table 8.5). Without incorporating both Nb and pyridine into the HPA precursor, ethane conversions were only 0.1%. No acetic acid was observed, and the samples produced mostly CO_x (68-85%, with the balance ethylene). It was only in a Nb- and pyridine-exchanged HPA that ethane conversion and selectivity to acetic acid was observed at elevated pressure.

8.3.2 Study of $Nb_{0.4}PMo_{12}$pyr in Atmospheric Pressure Ethane Reactions

The ethane oxidation reaction was then examined at atmospheric pressure for $NbPMo_{12}$pyr, having flow rates of 16: 8: 16: *x* mL/min ethane: oxygen: helium: steam, where *x* was varied from 0 to 20. Again, 0.6 mL of catalyst was used to have a GHSV of 6000 hr^{-1}, comparable to the pressurized reactions and retaining the ethane to oxygen ratio of 2:1. Without steam, ethane conversion was 30.5%, but 65.1% of the products formed were CO_x (see Figure 8.11). The selectivity to ethylene and acetic acid was 34.4% and 0.6%, respectively. Increasing amounts of steam flow in the feed improved the selectivity to ethylene and acetic acid, by decreasing the conversion to 18.1%. The gain in acetic acid was greater; acetic acid selectivity increased to 14.0% with 20 mL/min of steam fed. The STY of acetic acid increased from 0.002 to 0.021 mmol/min/g catalyst as the steam feed increased from 0 to 20 mL/min (see Figure 8.12) However, the improvement observed still was caused by the change in conversion, as seen in the plot of selectivity vs. conversion in Figure 8.13. No optimal steam feed rate was observed at atmospheric pressure.

The effect of reaction temperature was studied at atmospheric pressure at flow rates of 16: 8: 16: 20 mL/min of ethane: oxygen: helium: steam (see Table 8.6). Decreasing the temperature from 380 to 300^{o}C dropped the ethane conversion from 18.1 to 3.1%. For the same temperature change, the selectivity to CO_x decreased from 38.1 to 10.6%. Ethylene and acetic acid selectivity improved from 47.8 and 14.0%, respectively, at 380^{o}C, to 57.3 and 32.1% at 300^{o}C. However, no gain in STY of either ethylene or acetic acid was observed because of the decrease in conversion (see Figure 8.14).

It is important to note that all of the data discussed so far was measured on the high pressure reactor, regardless of the reaction pressure studied. The effect of Nb and pyridine on catalyst performance at atmospheric pressure was studied on the low pressure reactor system. In order to properly compare results between the two different reactor systems, a duplicate reaction of $NbPMo_{12}$pyr at 380^{o}C, 0 psig and flows of 16: 8: 16: 20 mL/min ethane: oxygen: helium: steam was performed to compare with the results obtained using the high pressure reactor (see Table 8.7). The ethane conversion was only slightly lower between the two reactors (18.1 and 15.3% conversion on the high and low pressure system, respectively). Product selectivity, however, was not similar in the two systems. More CO_x was observed in the low pressure reactor (57.1% vs. 38.1%) than on the high pressure reactor. As a result, less ethylene was observed (39.1% vs. 47.8%). The ethylene STY was only 0.050 mmol/min/g catalyst on the low pressure reactor, compared to 0.072 mmol/min/g catalyst.

The most striking difference between the reactor systems was the change in acetic acid observed. The production of acetic acid dropped an order of magnitude in the low pressure reactor. On the high pressure reactor, 14.0% selectivity to acetic acid was

observed; at the same conditions on the low pressure reactor, only 3.8% selectivity to acetic acid was found. This change was reflected in the drop in STY of acetic acid. The low pressure reactor measured only 0.005 mmol/min/g catalyst, instead of the 0.021 mmol/min/g catalyst found by the high pressure reactor.

Various possibilities were explored to explain these observations, such as GC/MS calibration, equipment contamination, hot spots in the reactor tube (see Figure A.5 in Appendix A) and catalyst source. No definitive explanation of the difference has yet been discovered, although efforts are continuing. Several differences between the two reactor configurations are being explored. On the high pressure reactor the gas feeds are mixed through a set of mixing coils contained within the heated reactor cabinet (see Figure 8.5A). Liquid water is also fed into one of these coils. A gas feed (helium) sweeps through the entrance of liquid water to the mixing assembly, to assist in the evaporation and dispersal of steam. All four streams are allowed to thoroughly heat and then mix at a tee prior to the entrance of the reactor.

Water is introduced differently in the low pressure reactor (see Figure 8.5B). The three gas streams are fed into the same mixing coils inside of the heated reactor cabinet. However, the combined gas stream then *exits* the reactor cabinet to sweep through the bottom of a ⅜-inch stainless steel tube filled with glass beads and heated to 170^{o}C. Liquid water is fed to the bottom of the bead-filled tube. The gases should sweep the water into the tube for vaporization and mixing. From the top of the mixing tube, the reactant stream is fed into the reactor tube. Dissolved catalyst has occasionally been observed in the liquid product trap during reaction studies, even at steady state. It may be that some of the water is not completely vaporized and mixed with the gas stream in the

bead-filled tube. The presence of liquid water may affect the stability of the catalyst active phase and cause deactivation, increasing the selectivity to CO_x in the low pressure reactor.

The high pressure reactor also has a multi-port valve upstream of the reactor to allow the feed stream to bypass the reactor tube. This feature enables one to begin reactant flow while using the reactor bypass to allow time for the gas streams (especially the steam) to start up without entering the catalyst bed. The streams can then be sent into the reactor tube after coming to steady state. The low pressure reactor does not currently have this feature, and the reactant stream must go directly into the reactor tube during feed startup. Combined with the possible inefficiency of the bead-filled mixing tube for the water vaporization, it is likely that incomplete water vaporization, especially during reactor startup, causes catalyst deactivation. Because of the inconsistency in feed configuration between the two reactors, some of the reaction data presented can only be used for identifying trends in catalyst activity. The product selectivity distribution and STY of products will be discussed, but conclusions should be made with caution.

The oxidation reaction was performed at 280^{o}C and 0 psig (on the low pressure reactor) at flow rates of 8: 4: 25: 10 mL/min in order to compare to the results at elevated pressure on the high pressure reactor (see Table 8.7). Changing the pressure from atmospheric to 230 psig at 280^{o}C increased the ethane conversion from 2.0% to 6.0%. The selectivity to CO_x increased from 24.8 to 64.5%, while the ethylene selectivity decreased from 61.6% to 23.2%. Acetic acid selectivity remained about the same (compare 13.5% and 12.4%). Ethylene STY was the same at both pressures, 0.006 mmol/min/g catalyst. Acetic acid production was slightly improved under pressure at

0.003 mmol/min/g catalyst, instead of 0.001. It may be that the advantage of performing the ethane oxidation at atmospheric pressure is in part that higher reaction temperatures could be achieved without the homogeneous gas phase reaction becoming dominant. However, because the 280°C and 0 psig experiment was done on the low pressure reactor, which appeared to have artificially low selectivities to ethylene and acetic acid, the STYs of ethylene and acetic acid may be lower than what would have been obtained on the high pressure reactor configuration at atmospheric pressure and 280°C. This should be investigated to see if atmospheric pressure reactions are in fact more selective to acetic acid than at elevated pressure.

PMo_{12}, $NbPMo_{12}$, and PMo_{12}pyr were used as catalyst precursors for reaction at 380°C, 0 psig, and flows of 16: 8: 16: 20 mL/min ethane: oxygen: helium: steam on the low pressure reactor (see Table 8.8). Little ethane conversion was noted in the PMo_{12}, $NbPMo_{12}$, and PMo_{12}pyr samples (0.1 to 0.6%). No acetic acid was formed for PMo_{12} and PMo_{12}pyr at atmospheric pressure, as seen under pressurized conditions (see Table 8.5). This is different than the results reported by Ueda and co-workers, who found some acetic acid formed with PMo_{12}pyr at atmospheric pressure (10% selectivity at 1% ethane conversion).[5] This discrepancy could be due to differences in catalyst performance on the low pressure reactor, which has consistently reported lower acetic acid production than expected. PMo_{12} produced only CO_x as products. $NbPMo_{12}$ did have 8.2% selectivity to acetic acid and 52.8% to ethylene (the balance was CO_x), which was not observed in the pressurized runs. The formation of an active catalyst for ethane oxidation at atmospheric pressure required the combination of both Nb and pyridine in the exchanged HPA precursor.

Because the presence of Nb was found to be critical in the precursor HPA, the effect of Nb loading per Keggin unit was examined at 380°C, 0 psig, and flows of 16: 8: 16: 20 mL/min. The study of Nb loading in $NbPMo_{12}$pyr samples was performed entirely on the low pressure reactor. As seen in Table 8.8, ethane conversion was only 0.6% for PMo_{12}pyr (Nb/Keggin ratio = 0). No acetic acid was formed, and selectivity to CO_x was 69.5%. The addition of a small amount of Nb (0.04 Nb/Keggin) did not affect the ethane conversion significantly (0.9%). The product selectivity was altered (see Figure 8.15). The selectivity to CO_x dropped to 37.5% as ethylene selectivity increased to 55.5%. Acetic acid was also observed, at 7.1% selectivity. For Nb/Keggin of 0.2, CO_x selectivity continued to drop (34.2%) and ethylene increased (61.1%), but selectivity to acetic acid decreased (4.6%). The ethane conversion continued to improve as a function of Nb/Keggin loading, until a maximum at Nb/Keggin = 0.4 (15.3%). The conversion gradually then decreased with increased Nb/Keggin ratio. Ethylene selectivity, after dropping at Nb/Keggin of 0.4, continued to increase up to Nb/Keggin of 1.0. The STY of ethylene increased as a function of Nb loading, up to a maximum of 0.092 mmol/min/g catalyst at a loading of 0.8 (see Figure 8.16). Acetic acid STY was greater for the higher Nb loadings, having a maximum of 0.007 mmol/min/g catalyst at Nb/Keggin of 0.8 and 1.0. Selectivity vs. conversion, in Figure 8.17, exhibited competition between conversion and selectivity to ethylene and acetic acid. The effect of conversion on acetic acid was less for the Nb loading series than for variations in other reaction parameters (e.g., steam feeds) on the high pressure reactor. The issues with the low pressure reactor performance may be dampening out effects of Nb content on product selectivity. It would be beneficial to further examine the effect of Nb loading on $NbPMo_{12}$pyr.

8.3.3 Study of $Nb_{0.68}PMo_{11}Vpyr$ in Ethane Reactions

Holles *et al*. found that the incorporation of vanadium into the Keggin HPA precursor was essential for selectivity in propane oxidation to acrylic acid.[1] $NbPMo_{11}Vpyr$ was prepared (by Holles and co-workers, as described previously) and used in ethane reactions, both at atmospheric pressure and at elevated pressure. Experiments were first conducted on the high pressure reactor system. $NbPMo_{11}Vpyr$ was studied at 280°C and 230 psig, with flows of 8: 4: 27: 10 mL/min of ethane: oxygen: helium: steam (see line 4 of Table 8.9). Under pressure 2.2% of ethane was converted by $NbPMo_{11}Vpyr$. The conversion for $NbPMo_{11}Vpyr$ was less than that obtained under the same conditions (on the same reactor) for $NbPMo_{12}pyr$, at 6.0% (see line 4 of Table 8.7). The vanadium-substituted catalyst had lower selectivity to CO_x (40.3% instead of 64.5% for $NbPMo_{12}pyr$). This resulted in a higher selectivity to ethylene for $NbPMo_{11}Vpyr$ (46.8% instead of 23.2% for $NbPMo_{12}pyr$). No change was observed in acetic acid selectivity (13.0% for $NbPMo_{11}Vpyr$ and 12.4% for $NbPMo_{12}pyr$). STY of ethylene was higher for the vanadium-substituted catalyst at 0.008 mmol/min/g catalyst, instead of 0.006, due to improved selectivity. STY of acetic acid was slightly lower for $NbPMo_{11}Vpyr$ at 0.002 mmol/min/g catalyst, instead of 0.003, because of lower conversion. At elevated pressure the addition of vanadium into the Keggin precursor primarily improved selectivity to ethylene over CO_x, but did not affect the formation of acetic acid.

$NbPMo_{11}Vpyr$ was also run at atmospheric pressure (on the high pressure reactor system) and 380°C, with flows of 16: 8: 16: 20 mL/min ethane: oxygen: helium: steam and a GHSV of 6000 hr^{-1}. An ethane conversion of 15.5% was observed (see Table 8.9,

line 1) and 31.0% selectivity to acetic acid. Note that the $NbPMo_{12}pyr$, under the same conditions on the high pressure reactor, had only 14.0% selectivity to acetic acid at 18.1% ethane conversion (compare line 1 of Table 8.9 with line 1 of Table 8.7). The STY of acetic acid was increased from 0.021 (for $NbPMo_{12}pyr$) to 0.062 mmol/min/g catalyst for $NbPMo_{11}Vpyr$. The addition of vanadium into the Keggin precursor had a favorable affect on the acetic acid formation at atmospheric pressure, although not as significant as that observed in propane (only CO_x was formed from propane in the absence of vanadium). $NbPMo_{12}pyr$ had higher selectivity to both CO_x (38.1%) and ethylene (47.8%). $NbPMo_{11}Vpyr$ had selectivity to CO_x of 32.7% and to ethylene of 36.2%, because of the increased formation of acetic acid.

When measurement inconsistencies were found using $NbPMo_{12}pyr$ at atmospheric pressure on the low pressure reactor compared to the high pressure reactor (comparing lines 1 and 2 on Table 8.7, as discussed previously), repeat studies of the $NbPMo_{11}Vpyr$ reactivity at atmospheric pressure on the low pressure reactor was done. Comparing lines 1 and 2 on Table 8.9, a decrease in the conversion was observed on the low pressure reactor (9.4%) from the high pressure reactor (15.5%). Note that line 2 of Table 8.9 was done with only 0.3 mL of catalyst. Flows were adjusted accordingly to maintain the same GHSV. A greater selectivity to CO_x was observed on the low pressure reactor, as seen with $NbPMo_{12}pyr$, (46.0 instead of 32.7%). More ethylene was observed for $NbPMo_{11}Vpyr$ on the low pressure reactor (49.0% instead of 36.2%), reflected in the significantly decreased formation of acetic acid (5.0% instead of 31.0%). The decrease in acetic acid was observed for $NbPMo_{12}pyr$ also when comparing the low pressure reactor with the high pressure reactor, although the conversion difference was less (18.1% on the

high pressure reactor vs. 15.3% on the low pressure reactor for $NbPMo_{12}pyr$). The decrease in acetic acid selectivity was reflected in an order of magnitude lower STY of acetic acid on the low pressure reactor, 0.006 mmol/min/g catalyst, instead of 0.062.

The two catalysts, $NbPMo_{12}pyr$ and $NbPMo_{11}Vpyr$, should also be compared at atmospheric pressure using the data from the low pressure reactor (compare line 2 from Table 8.7 with line 2 from Table 8.9). On the low pressure reactor, $NbPMo_{11}Vpyr$ still had reduced ethane conversion than $NbPMo_{12}pyr$ (9.4% compared to 15.3%). The selectivity to CO_x was also reduced in the vanadium-substituted sample (46.0% vs. 57.1%). More ethylene was observed for $NbPMo_{11}Vpyr$ (49.0%) than in $NbPMo_{12}pyr$ (39.1%), unlike the high pressure reactor, where the ethylene selectivity dropped from 47.8% to 36.2% with the addition of vanadium. The selectivity to acetic acid still increased in $NbPMo_{11}Vpyr$ tested on the low pressure reactor (5.0% compared to 3.4% for $NbPMo_{12}pyr$), but not as significantly. Thus, the acetic acid STY increased slightly for $NbPMo_{11}Vpyr$ to 0.006 mmol/min/g catalyst from 0.004 with $NbPMo_{12}pyr$. It is speculated that some factor inherently different in the design of the two reactors is responsible for the inconsistency in performance for the same catalyst at the same conditions. This difference resulted in decreased catalyst activity (conversion) and increased CO_x formation by over-oxidation of the acetic acid (and some ethylene) formed. Feeding an acetic acid solution into the reactor tube containing silicon carbide, at reaction conditions (380^{o}C, 16: 8: 16: 20 mL/min ethane: oxygen: helium: steam, where the steam is from a dilute aqueous acetic acid solution of known concentration) showed that no contamination or hot-spot in the reactor tube was causing the acetic acid to over-oxidize to CO_x in the absence of a catalyst.

To compare the difference between atmospheric pressure and elevated pressure for $NbPMo_{11}Vpyr$, ethane reaction was done on the low pressure reactor at 280°C and atmospheric pressure (compare lines 3 and 4 on Table 8.9). Note that the 230 psig experiment was performed on the high pressure reactor. The ethane conversion increased slightly, from 1.1 to 2.2% as the pressure was increased from 0 to 230 psig at 280°C. Selectivity to CO_x increased from 29.9 to 40.3% with increased pressure. Ethylene and acetic acid selectivity both decreased with increased pressure, from 51.3 and 18.7%, respectively, to 46.8 and 13.0%, respectively. The STY of ethylene and acetic acid were slightly higher under pressure, at 0.008 and 0.002 mmol/min/g catalyst, respectively, because of higher conversion.

The effect of Nb loading in vanadium-containing catalysts was examined on the low pressure reactor, at 380°C and atmospheric pressure (see Figure 8.18). The catalyst loading was 0.3 mL, so reduced flow rates of 8: 4: 8: 10 mL/min of ethane: oxygen: helium: steam were used to maintain the same GHSV. Note that the catalyst samples used were exchanged by Holles and co-workers using $PMo_{11}V$ prepared by Holles and $NbCl_5$. No $PMo_{11}Vpyr$ sample, Nb/Keggin = 0, was available from those preparations for comparison. Results from $PMo_{12}pyr$ and extrapolation from Figure 8.18 suggest that a $PMo_{11}Vpyr$ sample would have little activity. At a Nb/Keggin loading of 0.04, only 1.0% ethane was converted. The conversion increased with increasing Nb loading, to 9.4% at Nb/Keggin = 0.68. (Note that this was the same sample loading that produced 15.5% conversion at these conditions in the high pressure reactor.) Further increases of Nb past 0.68 resulted in a decrease in conversion. In the range of Nb/Keggin of 0.12 to 0.87, product distribution remained constant, regardless of conversion, at approximately

45% CO_x, 49% ethylene, and 6% acetic acid. The 0.04 and 0.97 samples both showed increased selectivity to ethylene and decreased amounts of CO_x and acetic acid. In spite of the similar selectivities, changes in conversion due to Nb loadings greatly affected the STY of ethylene and slightly increased the STY to acetic acid (see Figure 8.19). The maximum in both was observed at a Nb/Keggin of 0.87, with STYs of 0.086 and 0.009 mmol/min/g catalyst of ethylene and acetic acid, respectively. This was the highest STY of acetic acid measured on the low pressure reactor. This suggests that out of all the various parameters and catalyst compositions studied, $Nb_{0.87}PMo_{11}Vpyr$ should have the highest production of acetic acid. The changes in selectivity as a function of conversion (Figure 8.20) were less dominant in the $NbPMo_{11}Vpyr$ series than in the $NbPMo_{12}pyr$ series (Figure 8.17).

One may obtain $PMo_{11}V$ and ammonium niobium oxalate from commercial sources instead of preparing the Keggin synthetically and using $NbCl_5$ as a precursor to niobium oxalate. Reactivity differences between the sample prepared by Holles and one prepared from commercial sources (both at Nb/Keggin = 0.68), were examined at atmospheric pressure on the low pressure reactor (see Table 8.10). The product selectivity of the two samples was similar, at 46% CO_x, 50% ethylene, and 4% acetic acid. The conversion was higher for the catalyst prepared from commercial sources than the Holles material (15.7% vs. 9.4%) on the low pressure reactor. Because of the higher conversion, STYs of ethylene and acetic acid were higher with the sample from commercial sources, 0.101 and 0.008 mmol/min/g catalyst, respectively. Because the Holles material performed better when measured on the high pressure reactor (15.5% conversion), it would be desirable to measure the performance of the sample prepared

from commercial sources under the same reactor configuration, preferably at a Nb/Keggin loading of about 0.87. Efforts are underway to change the configuration in the low pressure reactor to be the same as the design of the high pressure reactor.

8.3.4 Study of $Nb_{0.4}PMo_{12}$pyr Reactivity at Other Flow Compositions

Because not all of the oxygen was being utilized in the ethane oxidation, the ethane/oxygen ratio was increased from 2:1 (see Table 8.11). At a ratio of 3:1, the ethane and oxygen conversions over $NbPMo_{12}$pyr decreased, from 15.3 to 6.4% and 47.7 to 36.8%, respectively (compare lines 1 and 2). The selectivity to acetic acid did increase to 7.3% from 3.8%, but this could simply be a conversion effect. No change in the STY of acetic acid was observed. At a ratio of 4:1, however the ethane conversion was 12.9%, having 77.2% oxygen conversion. Selectivity to acetic acid was 5.6%. The acetic acid STY was 0.008 mmol/min/g catalyst (compared to 0.005 for 2:1 ethane/oxygen ratio), suggesting that it may be possible to continue to increase acetic acid production by increasing the ethane/oxygen ratio even further. Similar work should be done with the $Nb_{0.87}PMo_{11}V$pyr, preferably made with commercial materials.

8.3.5 Ethane Reactivity with Metals Other Than Nb

Holles and co-workers exchanged other metal cations with pyridine into the PMo_{12} Keggin to determine if other metals had similar activity and selectivities in butane oxidation.[1] Although some metals (e.g., Ti and Mo) possessed activity in the butane oxidation to maleic acid, none performed as well as Nb. HPAs exchanged with other metals known to be active for ethane oxidation (Ta, Sb, and Zr) were also used as catalyst precursors in ethane oxidation. Catalyst precursors prepared by Holles and co-workers were measured for activity in the low pressure reactor, at 380^{o}C and 0 psig, for flow rates

of 16: 8: 16: 20 mL/min ethane: oxygen: helium: steam. As seen in Table 8.12, some acetic acid was observed with each of the catalysts, but none of the other metals attempted (Ta, Sb, Zr, and Ti) had significant conversions of ethane (<2%). The butane system examined by Holles *et al*. exhibited more versatility with metal exchange than ethane. Nb has a special role in the formation of an active catalyst during pretreatment that cannot be duplicated for ethane oxidation.

8.3.6 Study of Ethylene Reactions with $Nb_{0.4}PMo_{12}pyr$

In order to probe the mechanism of formation of acetic acid from ethane, ethylene was used as a reactant feed. $NbPMo_{12}pyr$ was studies at 0 psig, at a range of temperatures, using 16: 8: 16: 20 mL/min of ethylene: oxygen: helium: steam as the feed mixture (see Table 8.13). At 380°C all of the oxygen was consumed, with an ethylene conversion of 28.0%. CO_x was the major product, at 76.7% selectivity, but acetic acid was also formed at 17.0% selectivity. Other products observed included acetaldehyde (AcAld, 0.58%), ethanol (EtOH, 0.04%), methyl acetate (MeAc, 0.02%), ethyl acetate (EtAc, 0.03%), acetone (0.17%), propanoic acid (0.05%), acrylic acid (3.7%), and maleic acid (1.7%).

Decreasing the temperature decreased the conversion and CO_x formation. At 240°C (note: D_2O was fed as the source of steam) ethane conversion was 1.8%. CO_x selectivity decreased to 64.5%. Acetic acid selectivity increased to 30.4%. The selectivity of acetaldehyde, ethanol, methyl acetate, and ethyl acetate all increased as the temperature decreased (to 1.1, 2.5, 0.31, and 1.1%, respectively, at 240°C). No acetone, propanoic acid, acrylic acid or maleic acid was observed at 240°C. This suggests that an ethoxy or acetate species might be involved in the formation of acetic acid from ethylene.

Tessier and Merzouki found acetic acid production to be dominant at low temperatures (250-300^{o}C) and ethylene production dominant at higher temperatures, suggesting two different reaction pathways.[6,7] Addition of steam improves the transformation of the adsorbed ethoxy species to acetic acid and then assists in the desorption.[8] Acetic acid formation is a balance between the selectivity at low conversion (low temperatures) and the desorption of the products from the surface (high temperatures). The selectivity to what may be primary products of ethane oxidation may be artificially low because the ethylene studies were done on the low pressure reactor. Further examination should be done on the mechanism of acetic acid formation from ethylene.

D_2O was used as the source of steam for the 240^{o}C reaction in order to probe the effect of water on acetic acid formation from ethylene. Mass spectroscopy was used to quantify the amount of deuterium substitution of the acetic acid observed. A distribution of d_0, d_1, d_2, and d_3 substitution was calculated by extraction of m/z = 60, 61, 62, and 63. The peak areas were integrated, giving substitution of 0.9% (d_0), 7.3% (d_1), 32.1% (d_2), and 59.6% (d_3), respectively. Clearly, the D_2O in the gas feed was involved in the formation of acetic acid. The low amount of d_0-acetic acid was likely due to the formation of H_2O as a result of ethane oxidation.

D_2O was eliminated from the feed to see if the removal of steam resulted in the increase of total oxidation products, CO_x. CO_x did increase, but less than expected. Ethylene conversion was similar to that with steam (1.7%), but there was a slight increase in CO_x production (71.9%). Deuterated acetic acid and liquid water were still observed even during the second hour after D_2O removal. Selectivities of the liquid oxygenates all decreased with the removal of steam, but they were still present. It may be that some

adsorbed surface species were still being desorbed from the catalyst, but it was surprising that any desorption would be still occurring during the second hour without steam. It is possible that some D_2O remained in the feed (due to poor mixing as previously discussed) even after the syringe pump was stopped that prolonged the exposure of the catalyst to D_2O.

8.4 References

(1) Holles, J. H. *et al., J. Catal.* **2003**, *218*, 42.

(2) Dillon, C. J. *et al., J. Catal.* **2003**, *218*, 54.

(3) Tsigdinos, G. A.; Hallada, C. J. *Inorg. Chem.* **1968**, *7*, 437.

(4) Davis, M. E. *et al., Angew. Chem., Int. Ed.* **2002**, *41*, 858.

(5) Li, W.; Ueda, W. *Stud. Surf. Sci. Catal.* **1997**, *110*, 433.

(6) Tessier, L. *et al., Catal. Today* **1995**, 335.

(7) Merzouki, M. *et al.,* In *New Frontiers in Catalysis*; Guczi, L., al., e., Eds.; Elsevier Science, 1993.

(8) Centi, G. *et al., Selective Oxidation by Heterogeneous Catalysis*; Kluwer Academic/Plenum Publishers: New York, 2001.

Figure 8.1 $Nb_xPMo_{12}pyr$, with varying Nb/Keggin ratios.

Figure 8.2 Phosphomolybdic acid and its niobium- and pyridine-exchanged forms.

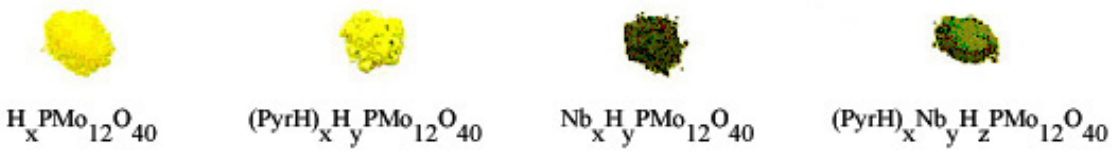

Figure 8.3 Phosphovanadomolybdic acid and its niobium- and pyridine-exchanged forms.

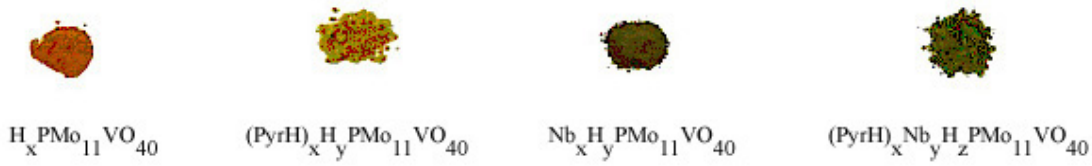

$H_xPMo_{11}VO_{40}$ $(PyrH)_xH_yPMo_{11}VO_{40}$ $Nb_xH_yPMo_{11}VO_{40}$ $(PyrH)_xNb_yH_zPMo_{11}VO_{40}$

Figure 8.4 $Nb_xPMo_{11}Vpyr$, with varying Nb/Keggin ratios.

0.04 0.12 0.3 0.68 0.87 0.98

Figure 8.5 Autoclave Engineers BTRS, Jr. reactor schematics: (A) high pressure reactor system and (B) low pressure reactor system.

(A)

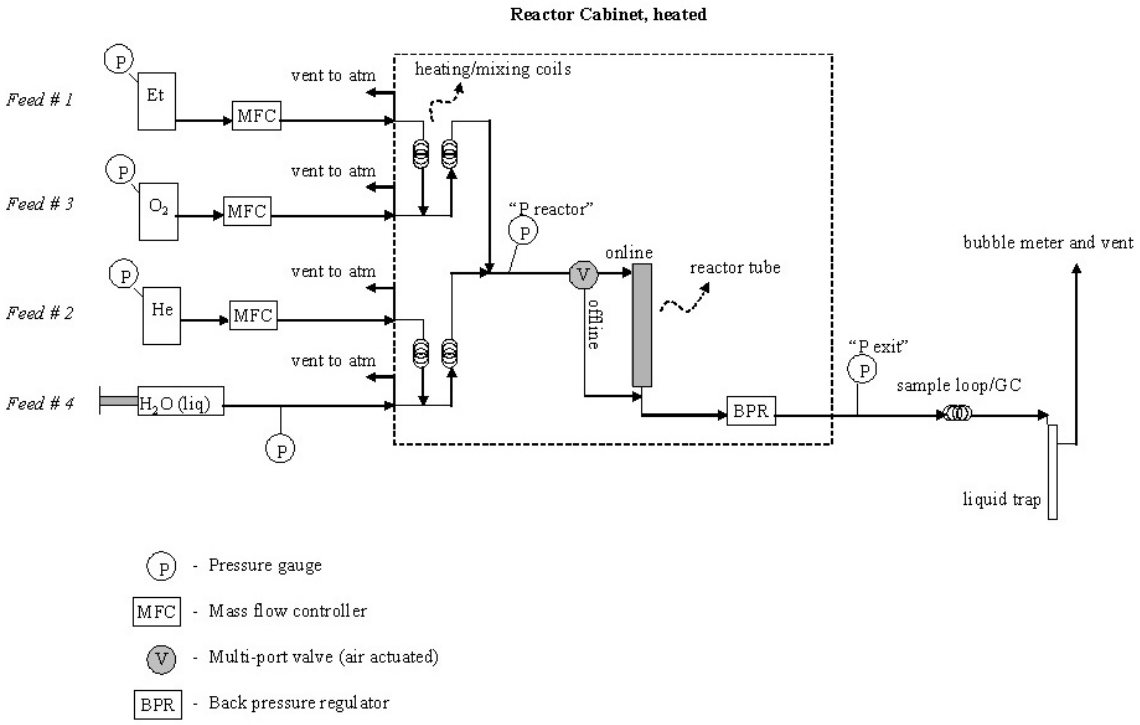

(B)

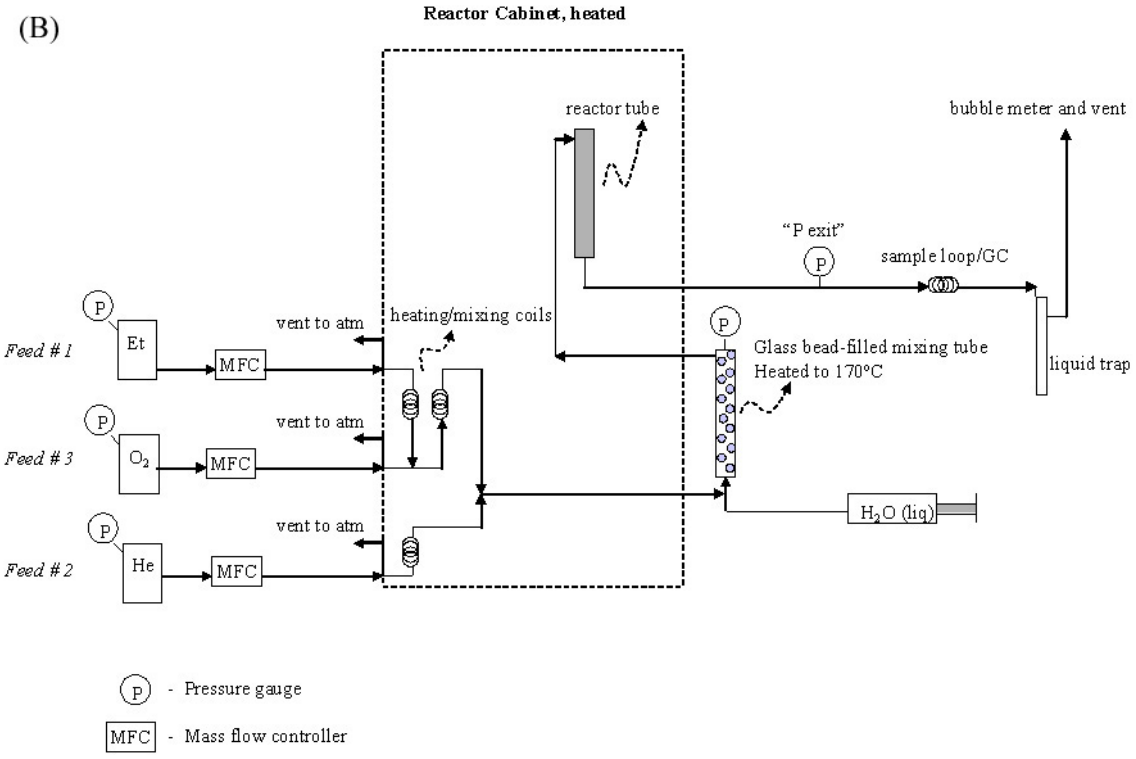
Reactor Cabinet, heated
reactor tube
bubble meter and vent
"P exit"
P
sample loop/GC
P
Et
MFC
vent to atm
heating/mixing coils
Feed # 1
Glass bead-filled mixing tube
Heated to 170°C
liquid trap
P
O2
MFC
vent to atm
Feed # 3
H2O (liq)
P
He
MFC
vent to atm
Feed # 2
P - Pressure gauge
MFC - Mass flow controller

Figure 8.6 Ethane reactivity of $NbPMo_{12}pyr$ at 280°C, 230 psig, 8: 4: 27: *x* mL/hr (ethane: oxygen: helium: steam) on high pressure reactor.

Data listed in Table C.1

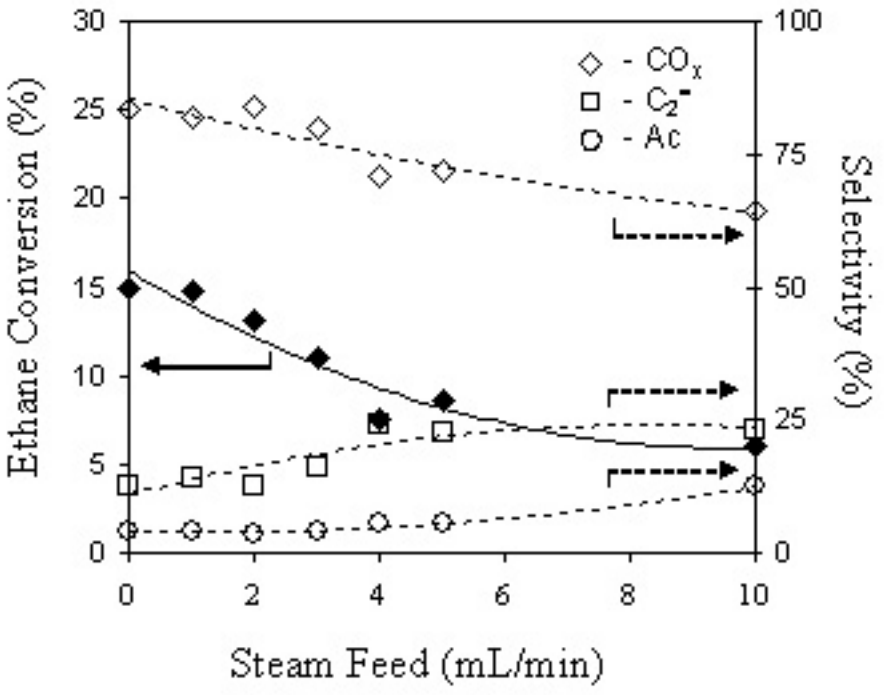

Figure 8.7 Space time yield of products for $NbPMo_{12}pyr$ at 280°C, 230 psig, 8: 4: 27: *x* mL/hr (ethane: oxygen: helium: steam) on high pressure reactor.

Data listed in Table C.1

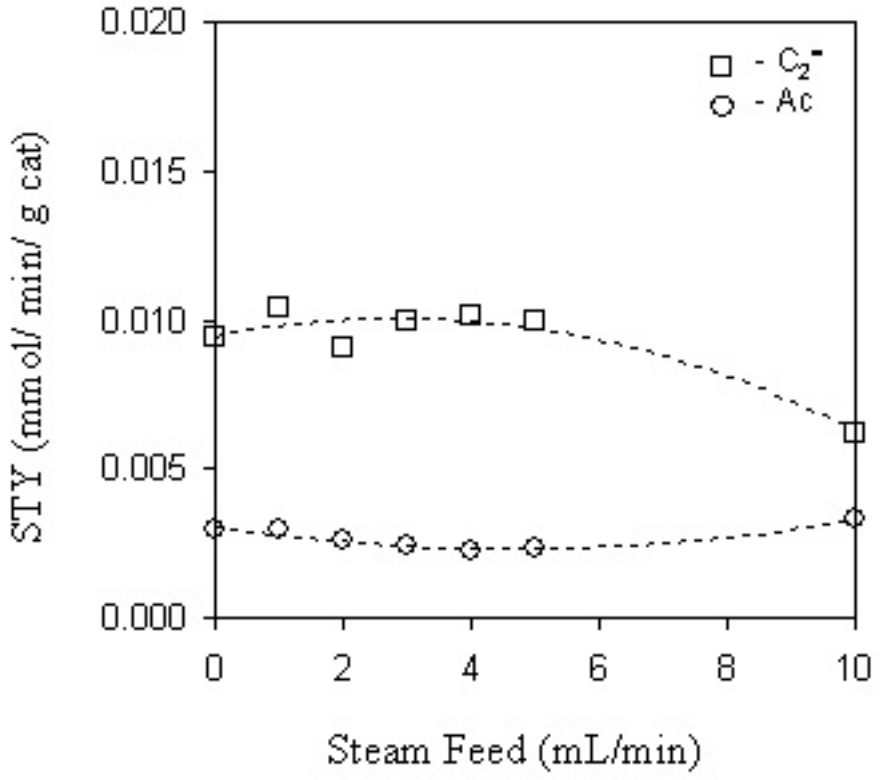

Figure 8.8 Selectivity vs. conversion for $NbPMo_{12}pyr$ at 280°C, 230 psig, 8: 4: 27: *x* mL/hr (ethane: oxygen: helium: steam) on high pressure reactor.

Data listed in Table C.1

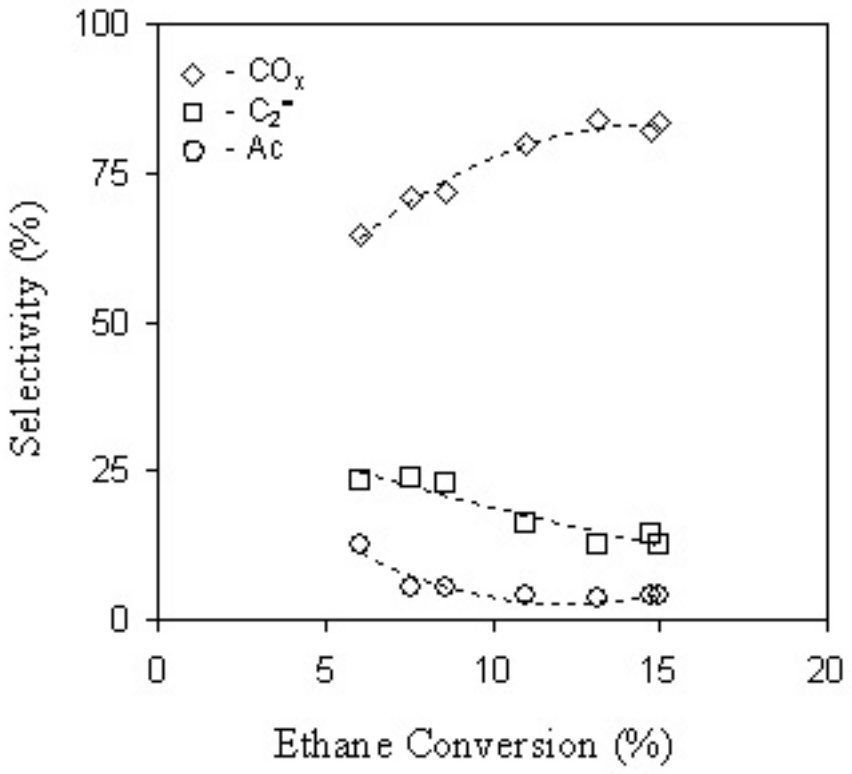

Figure 8.9 Ethane reactivity of $NbPMo_{12}pyr$ at 280°C, 230 psig, 8: 4: 27: 10 mL/hr (ethane: oxygen: helium: steam) on high pressure reactor. Catalyst volume was varied. *Data listed in Table C.2*

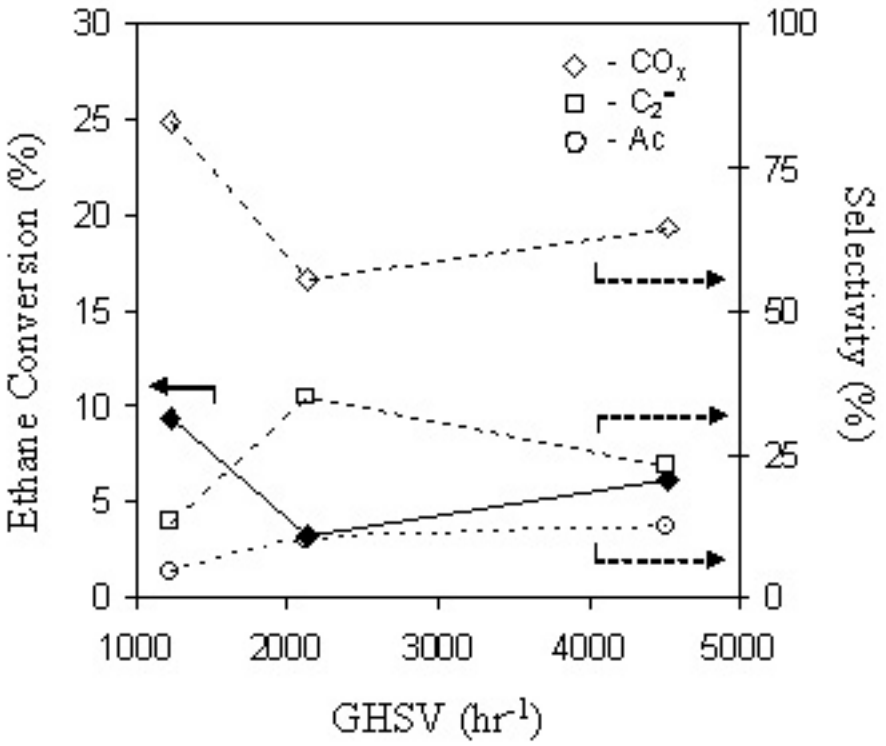

Figure 8.10 Space time yield of products for $NbPMo_{12}pyr$ at 280°C, 230 psig, 8: 4: 27: 10 mL/hr (ethane: oxygen: helium: steam) on high pressure reactor. Catalyst volume was varied.

Data listed in Table C.2

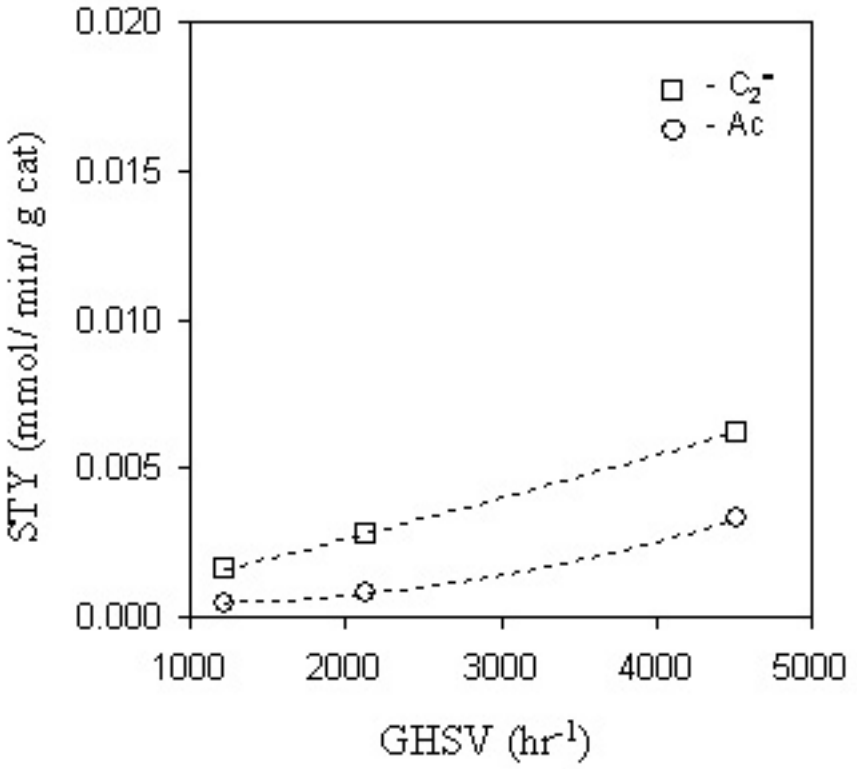

Figure 8.11 Ethane reactivity of $NbPMo_{12}pyr$ at 380°C, 0 psig, 16: 8: 16: *x* mL/hr (ethane: oxygen: helium: steam) on high pressure reactor.

Data listed in Table C.3

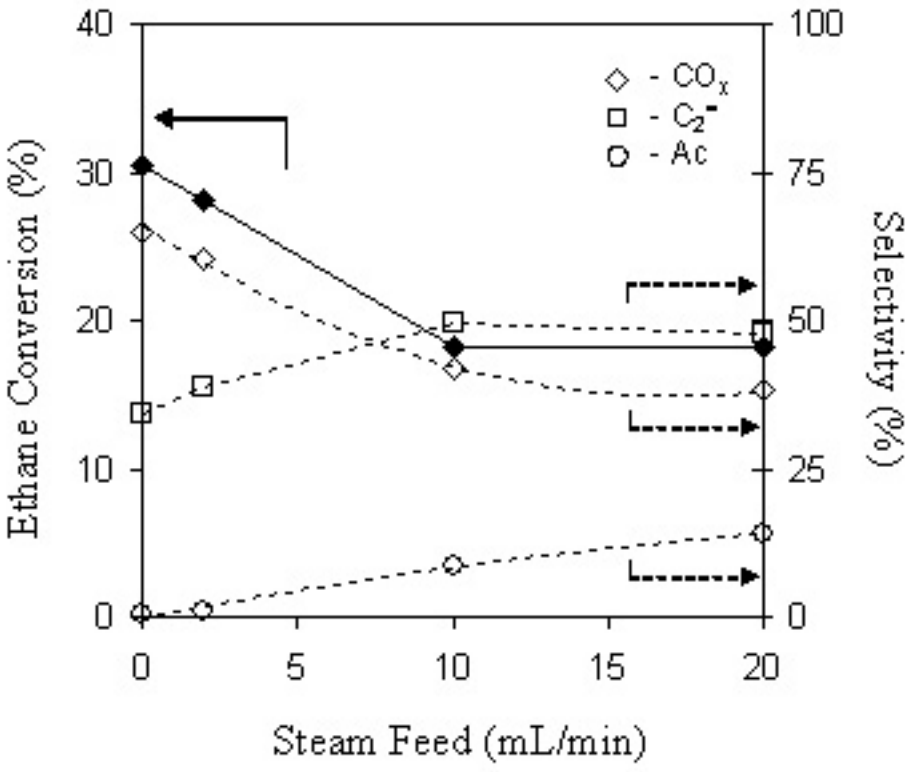

Figure 8.12 Space time yield of products for $NbPMo_{12}pyr$ at 380°C, 0 psig, 16: 8: 16: *x* mL/hr (ethane: oxygen: helium: steam) on high pressure reactor.

Data listed in Table C.3

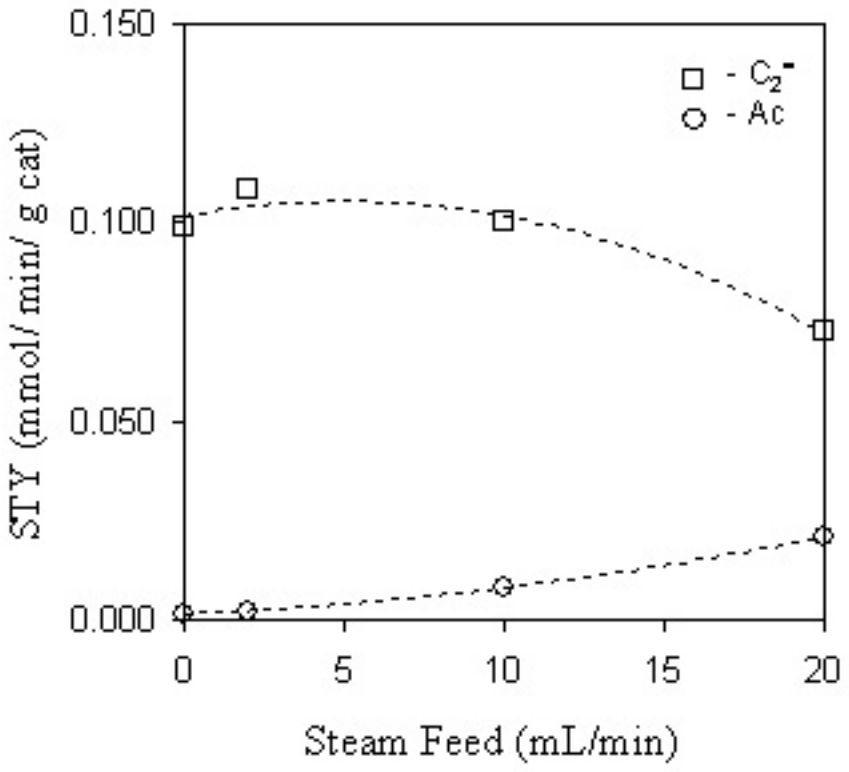

Figure 8.13 Selectivity vs. conversion for $NbPMo_{12}pyr$ at 380°C, 0 psig, 16: 8: 16: *x* mL/hr (ethane: oxygen: helium: steam) on high pressure reactor.

Data listed in Table C.3

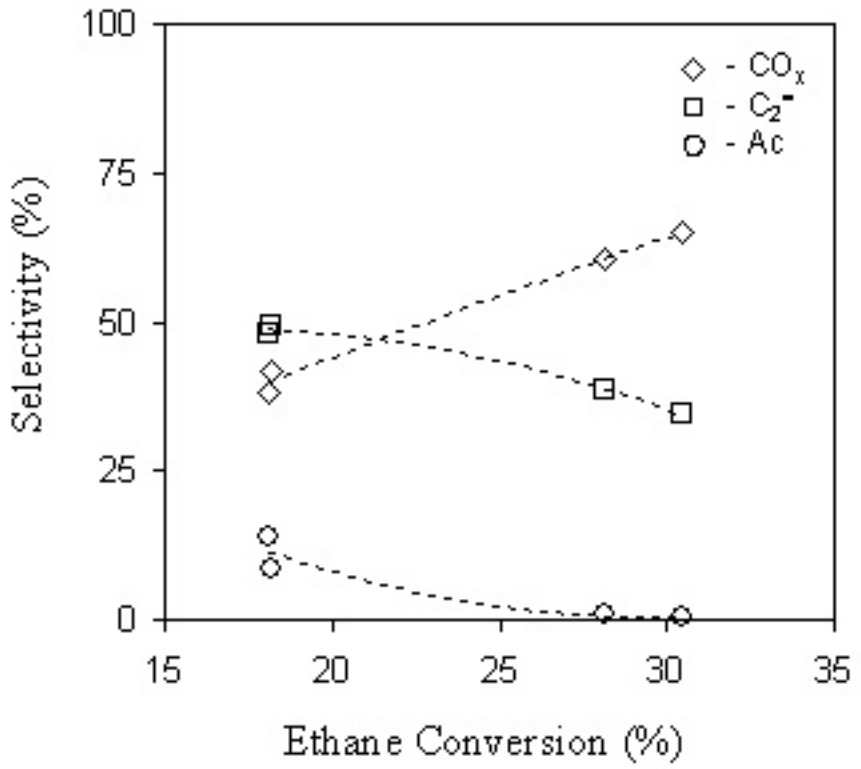

Figure 8.14 Ethane reactivity with temperature of $NbPMo_{12}pyr$ at 0 psig, 16: 8: 16: 20 mL/hr (ethane: oxygen: helium: steam) on high pressure reactor, except 280°C run on low pressure reactor.

Data listed in Table 8.6 and C.4

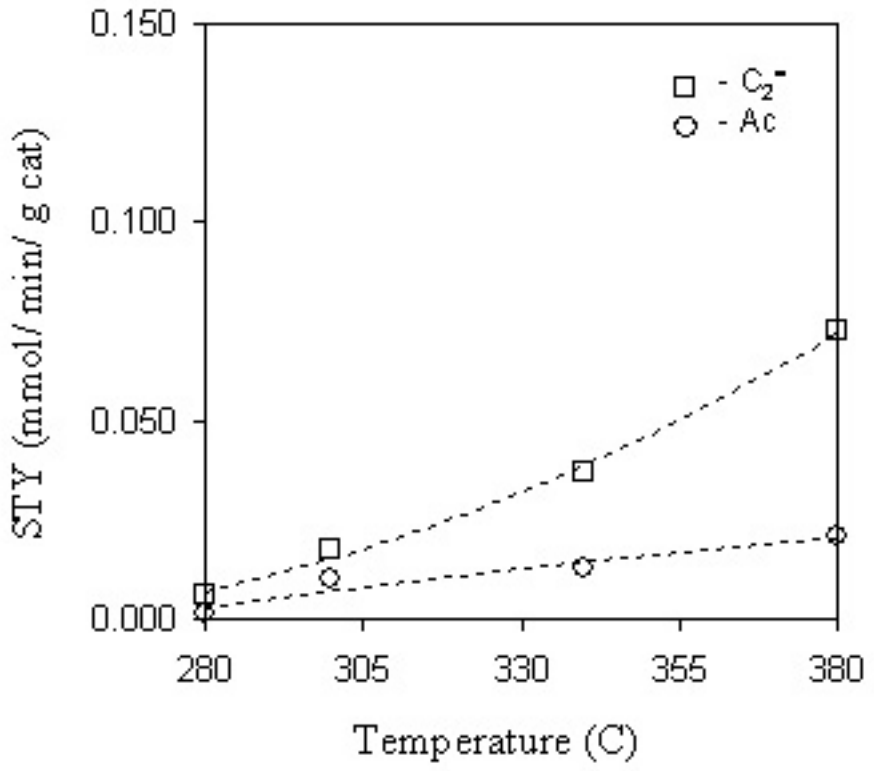

Figure 8.15 Ethane reactivity with Nb loading of $NbPMo_{12}pyr$ at 380°C, 0 psig, 16: 8: 16: 20 mL/hr (ethane: oxygen: helium: steam) on low pressure reactor.

Data listed in Table C.5

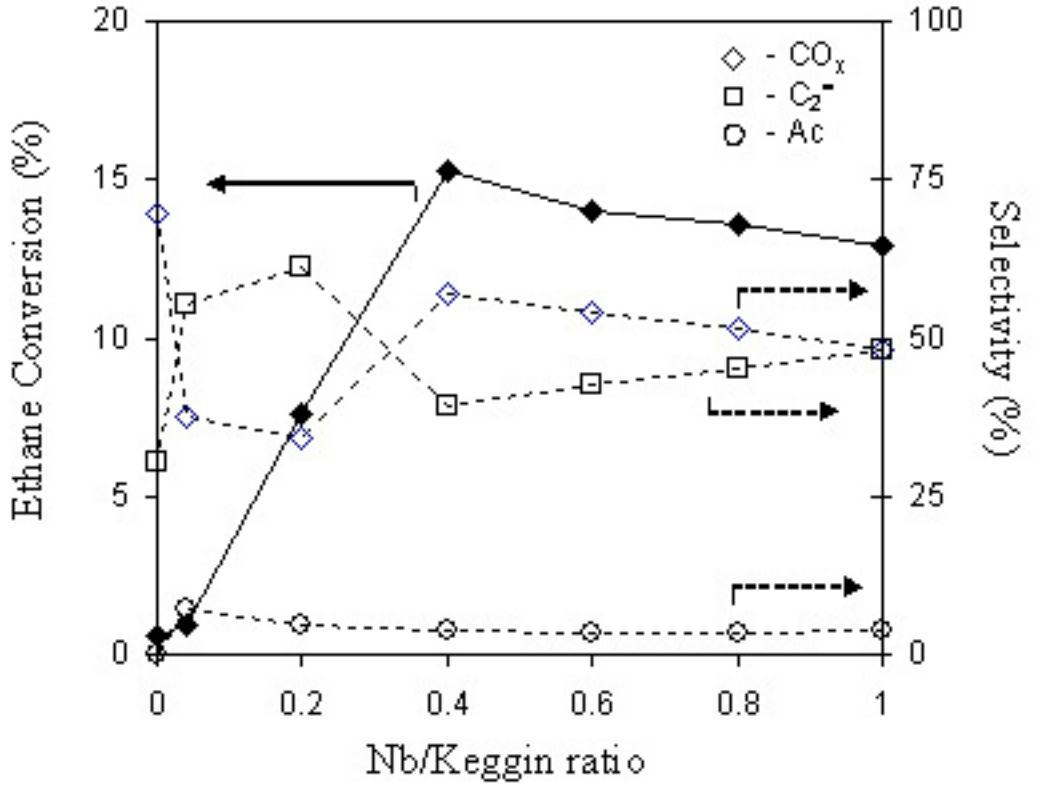

Figure 8.16 Space time yield of products for Nb loading of $NbPMo_{12}pyr$ at 380°C, 0 psig, 16: 8: 16: 20 mL/hr (ethane: oxygen: helium: steam) on low pressure reactor.

Data listed in Table C.5

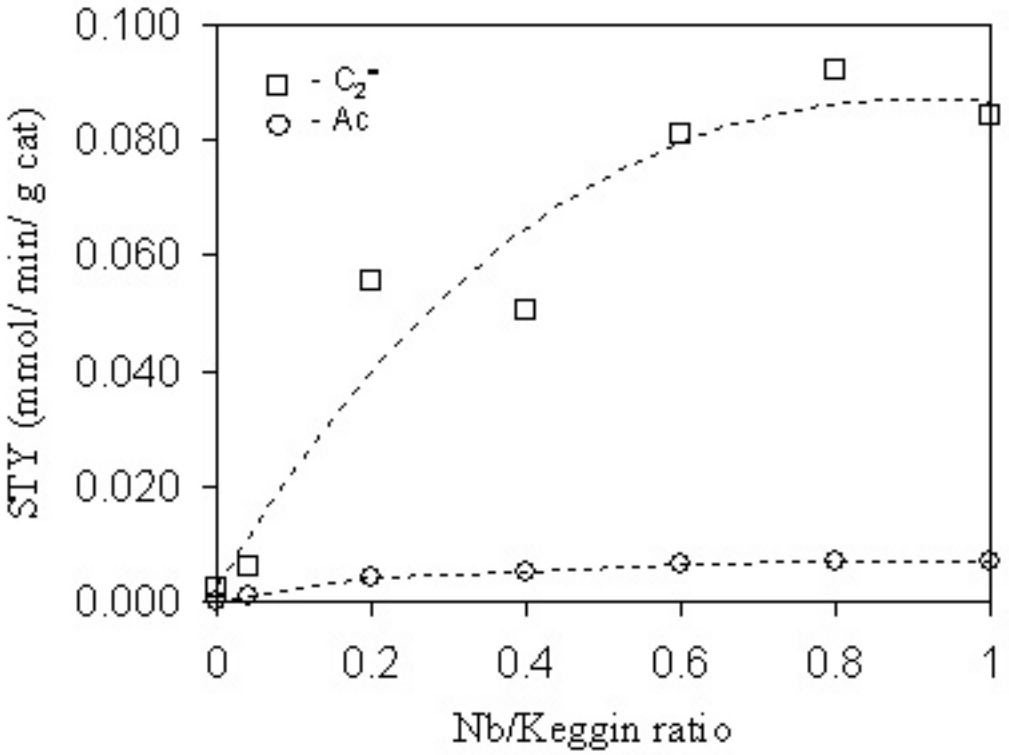

Figure 8.17 Selectivity vs. conversion for Nb loading of $NbPMo_{12}pyr$ at 380°C, 0 psig, 16: 8: 16: 20 mL/hr (ethane: oxygen: helium: steam) on low pressure reactor.

Data listed in Table C.5

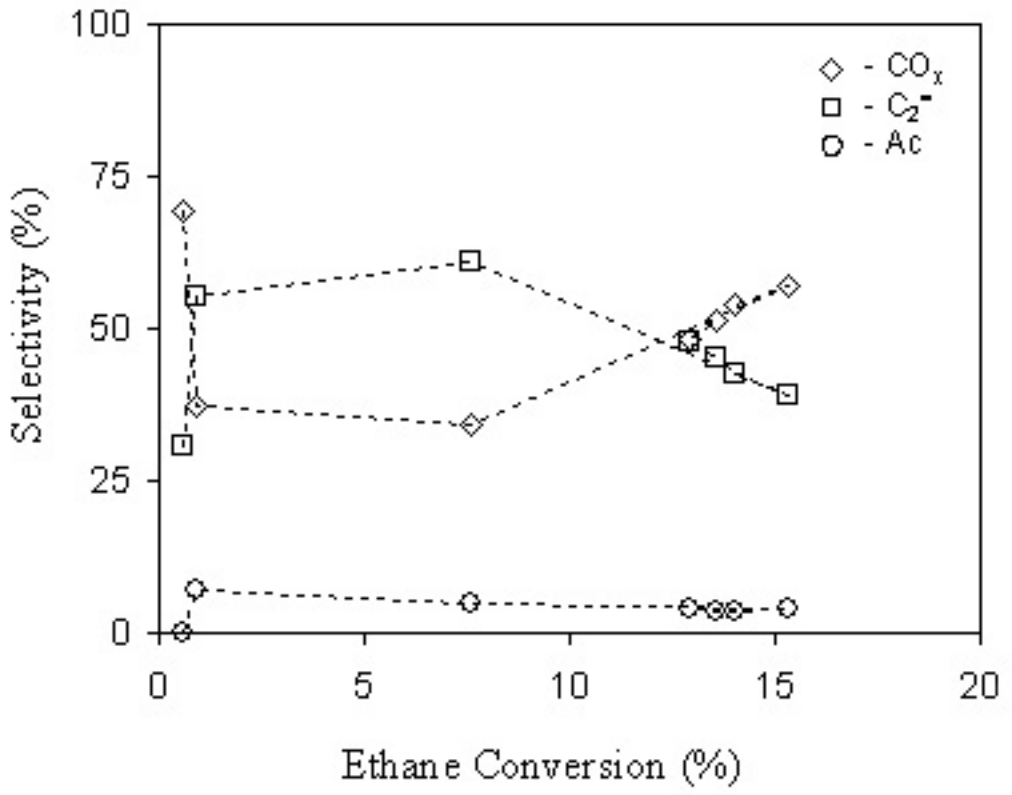

Figure 8.18 Ethane reactivity with Nb loading of $NbPMo_{11}Vpyr$ at 380°C, 0 psig, 8: 4: 8: 10 mL/hr (ethane: oxygen: helium: steam) on low pressure reactor, $V_{catalyst}$ = 0.3 mL.

Data listed in Table C.6

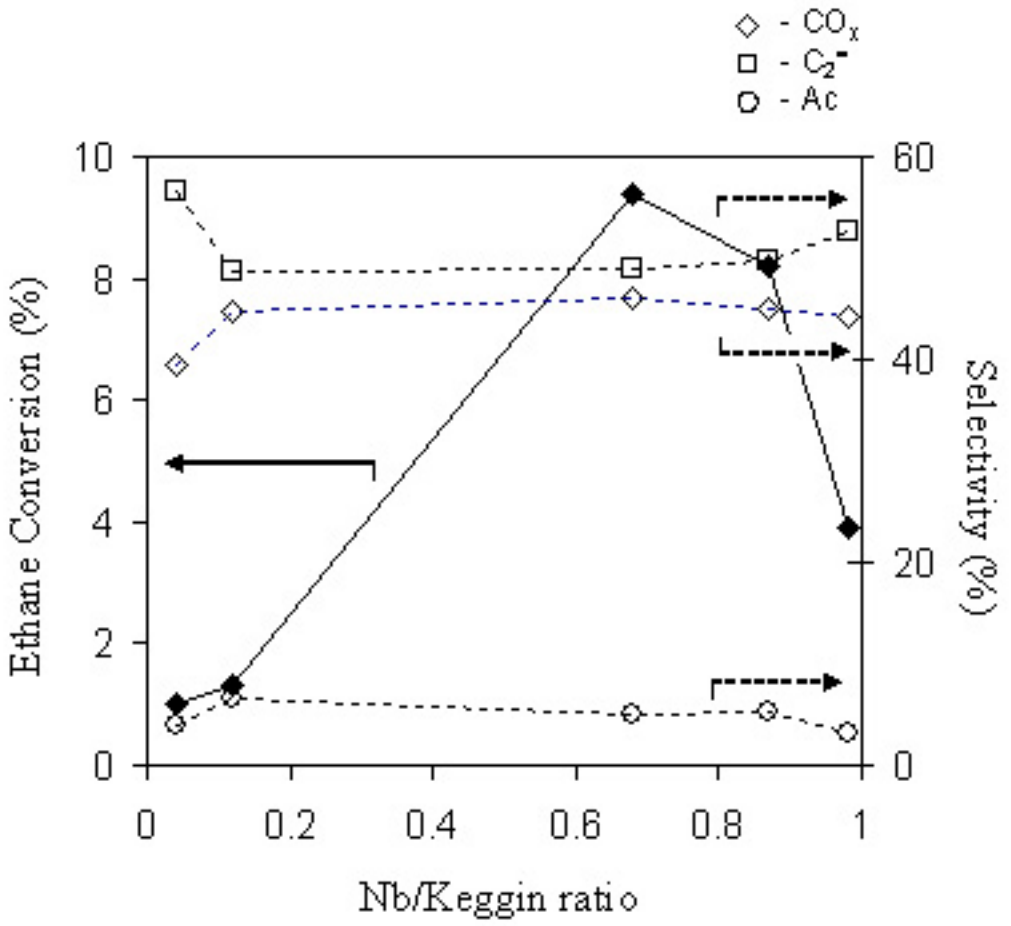

Figure 8.19 Space time yield of products for Nb loading of $NbPMo_{11}Vpyr$ at 380°C, 0 psig, 8: 4: 8: 10 mL/hr (ethane: oxygen: helium: steam) on low pressure reactor, $V_{catalyst}$ = 0.3 mL.

Data listed in Table C.6

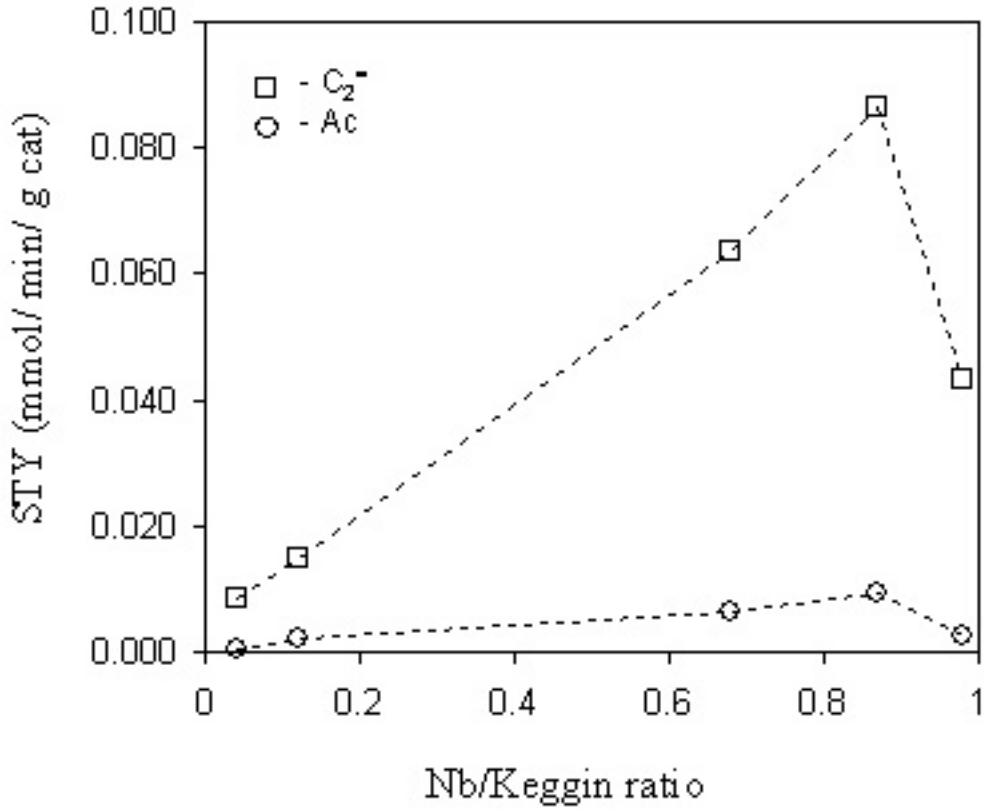

Figure 8.20 Selectivity vs. conversion for Nb loading of $NbPMo_{11}Vpyr$ at 380°C, 0 psig, 8: 4: 8: 10 mL/hr (ethane: oxygen: helium: steam) on low pressure reactor, $V_{catalyst}$ = 0.3 mL.

Data listed in Table C.6

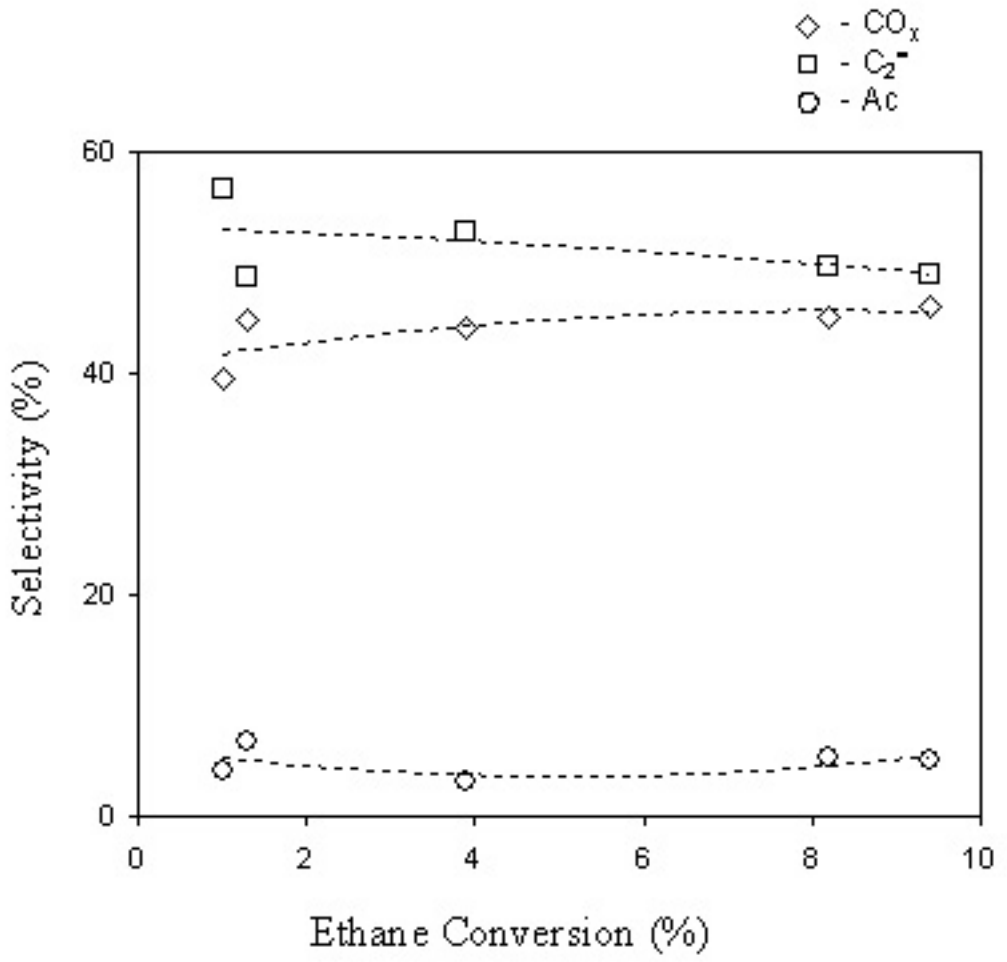

Table 8.1 *n*-Butane reactivity at 380°C. Adapted from ref. 1.

Catalyst	Flow	Conv.	Selectivity[a]				STY[b]
	C_4: O_2: He: H_2O	(%)	CO_x	Ac	AA	MA	MA
PMo_{12}	4: 2: 4: 5	0.2	64	34	2	0	0
$NbPMo_{12}$	4: 2: 4: 5	3	13	7	2	70	0.017
PMo_{12}pyr	4: 2: 4: 5	13.5	14	3	1	82	0.097
	32: 16: 32: 40	2.5	9	6	6	71	0.11
$NbPMo_{12}$pyr	4: 2: 4: 5	15	25	3	1	71	0.084
	32: 16: 32: 40	15	5	3	1	90	0.84
$PMo_{11}V$	4: 2: 4: 5	0.5	31	17	0	50	$1.6x10^{-3}$
$NbPMo_{11}V$	4: 2: 4: 5	0.4	42	19	4	25	$6.3x10^{-4}$
$PMo_{11}V$pyr	4: 2: 4: 5	13.5	5	3	1	90	0.11
$NbPMo_{11}V$pyr	4: 2: 4: 5	15	16	5	2	76	0.090
	32: 16: 32: 40	14	9	5	3	80	0.76

[a]Ac = acetic acid; AA = acrylic acid; MA = maleic acid

[b]STY is in mmol/min/g catalyst

Table 8.2 Propane reactivity at 380°C. Adapted from ref. 1.

Catalyst	Flow	Conv.	Selectivity[a]					STY[b]
	C_3: O_2: He: H_2O	(%)	CO_x	$C_3^=$	Ac	AA	MA	AA
$PMo_{11}V$	8: 4: 8: 10	0.4	30	54	4	0	0	0
$NbPMo_{11}V$	8: 4: 8: 10	1.4	22	44	16	10	0	$1.4x10^{-3}$
$PMo_{11}Vpyr$	8: 4: 8: 10	3.4	10	37	30	17	0	$5.5x10^{-3}$
$NbPMo_{12}pyr$	8: 4: 8: 10	25	79	1	2	2	14	0.008
$NbPMo_{11}Vpyr$	8: 4: 8: 10	25	15	-	19	21	43	0.18
	32: 16: 32: 40	21	11	0	23	49	15	0.62

[a] $C_3^=$ = propylene; Ac = acetic acid; AA = acrylic acid; MA = maleic acid

[b] STY is in mmol/min/g catalyst

Table 8.3 Temperature effects for $NbPMo_{12}pyr$ at 230 psig, 8: 4: 27: 10 mL/hr (ethane: oxygen: helium: steam) on high pressure reactor.

Temperature	Conversion			Selectivity		STY[a]	
(C)	C_2	O_2	CO_x	$C_2^=$	Acetic	$C_2^=$	Acetic
330	8.1	36.7	59.5	35.7	4.8	0.015	0.002
280	6.0	28.4	64.5	23.2	12.4	0.006	0.003
240	0.4	1.1	18.3	59.1	22.6	0.001	$4.0x10^{-4}$

[a]STY is in mmol/min/g catalyst

Table 8.4 Ethane reactivity of $NbPMo_{12}pyr$ at 280°C, 230 psig, (8: 4: 27: 0) mL/hr (ethane: oxygen: helium: steam) on high pressure reactor. Catalyst volume was varied.

GHSV (hr^{-1})	Conversion		Selectivity			STY[a]	
	C_2	O_2	CO_x	$C_2^=$	Acetic	$C_2^=$	Acetic
975	15.1	100	87.7	7.8	4.5	0.002	0.001
1638	20.4	100	90.3	6.3	3.4	0.003	0.002
3900	15.0	87.4	83.4	12.7	3.9	0.009	0.003

[a]STY is in mmol/min/g catalyst

Table 8.5 Ethane reactivity of PMo_{12}, $NbPMo_{12}$, PMo_{12}pyr, and $NbPMo_{12}$pyr at 280°C, 230 psig, 8: 4: 27: 10 mL/hr (ethane: oxygen: helium: steam) on high pressure reactor.

Catalyst	Conversion		Selectivity			STY[a]	
	C_2	O_2	CO_x	$C_2^=$	Acetic	$C_2^=$	Acetic
PMo_{12}	0.1	0.4	81.1	18.9	0	$6.5x10^{-5}$	0
$NbPMo_{12}$	0.1	0.4	67.9	32.1	0	$1.1x10^{-4}$	0
PMo_{12}pyr	0.1	0.7	84.6	13.4	0	$8.6x10^{-5}$	0
$NbPMo_{12}$pyr	6.0	28.4	64.5	23.2	12.4	0.006	0.003

[a]STY is in mmol/min/g catalyst

Table 8.6 Ethane reactivity with temperature of $NbPMo_{12}pyr$ at 0 psig, 16: 8: 16: 20 mL/hr (ethane: oxygen: helium: steam) on high pressure reactor.

Temperature	Conversion		Selectivity			STY[a]	
(C)	C_2	O_2	CO_x	$C_2^=$	Acetic	$C_2^=$	Acetic
380	18.1	46.1	38.1	47.8	14.0	0.072	0.021
340	6.5	14.0	21.7	59.1	19.2	0.037	0.012
300	3.1	6.5	10.6	57.3	32.1	0.017	0.010

[a]STY is in mmol/min/g catalyst

Table 8.7 Comparison of ethane reactivity of $NbPMo_{12}pyr$ between reactors and pressures. Reactor and flows used noted in table.

Temperature		Conversion			Selectivity		STY[a]	
(C)		C_2	O_2	CO_x	$C_2^=$	Acetic	$C_2^=$	Acetic
0 psig		Flow = 16: 8: 16: 20 mL/min (ethane: oxygen: helium: steam)						
380	high[b]	18.1	46.1	38.1	47.8	14.0	0.072	0.021
380	low[b]	15.3	47.7	57.1	39.1	3.8	0.050	0.005
0 psig		Flow = 8: 4: 25: 10 mL/min (ethane: oxygen: helium: steam)						
280	low[b]	2.0	6.3	24.8	61.6	13.5	0.006	0.001
230 psig		Flow = 8: 4: 27: 10 mL/min (ethane: oxygen: helium: steam)						
280	high[b]	6.0	28.4	64.5	23.2	12.4	0.006	0.003

[a]STY is in mmol/min/g catalyst

[b]Refers to the reactor used

Table 8.8 Ethane reactivity of PMo_{12}, $NbPMo_{12}$, PMo_{12}pyr, and $NbPMo_{12}$pyr at 380^{o}C, 0 psig, 16: 8: 16: 20 mL/hr (ethane: oxygen: helium: steam) on low pressure reactor.

Catalyst	Conversion		Selectivity			STY[a]	
	C_2	O_2	CO_x	$C_2^=$	Acetic	$C_2^=$	Acetic
PMo_{12}	0.1	0.9	100	0	0	0	0
$NbPMo_{12}$	0.3	0.9	39.0	52.8	8.2	0.002	$3.0x10^{-4}$
PMo_{12}pyr	0.6	2.8	69.5	30.5	0	0.002	0
$NbPMo_{12}$pyr	15.3	47.7	57.1	39.1	3.8	0.050	0.005

[a]STY is in mmol/min/g catalyst

Table 8.9 Comparison of ethane reactivity of $NbPMo_{11}Vpyr$ between reactors and pressures. Reactor and flows used noted in table.

Temperature		Conversion			Selectivity		STY[a]	
(C)		C_2	O_2	CO_x	$C_2^=$	Acetic	$C_2^=$	Acetic
0 psig		Flow = 16: 8: 16: 20 mL/min (ethane: oxygen: helium: steam)						
380	high[b]	15.5	40.8	32.7	36.2	31.0	0.075	0.062
		Flow = 8: 4: 8: 10 mL/min (ethane: oxygen: helium: steam), Vcat = 0.3 mL						
380	low[b]	9.4	32.6	46.0	49.0	5.0	0.064	0.006
0 psig		Flow = 4: 2: 12.5: 5 mL/min (ethane: oxygen: helium: steam), Vcat = 0.3 mL						
280	low[b]	1.1	4.4	29.9	51.3	18.7	0.003	0.001
230 psig		Flow = 8: 4: 27: 10 mL/min (ethane: oxygen: helium: steam)						
280	high[b]	2.2	8.0	40.3	46.8	13.0	0.008	0.002

[a]STY is in mmol/min/g catalyst

[b]Refers to the reactor used

Table 8.10 Comparison of ethane reactivity of (A) $NbPMo_{11}Vpyr$ prepared with $NbCl_5$ and synthetic Keggin and (B) $NbPMo_{11}Vpyr$ prepared with purchased Keggin and ammonium niobium oxalate, all on the low pressure reactor at a Nb/Keggin ratio of 0.68.

Temperature	Conversion		Selectivity			STY[a]	
(C)	C_2	O_2	CO_x	$C_2^=$	Acetic	$C_2^=$	Acetic
(A)	Flow = 16: 8: 16: 20 mL/min (ethane: oxygen: helium: steam)						
380	9.4	32.6	46.0	49.0	5.0	0.064	0.006
(B)	Flow = 8: 4: 8: 10 mL/min (ethane: oxygen: helium: steam), Vcat = 0.3 mL						
380	15.7	45.7	45.6	50.2	4.2	0.101	0.008

[a]STY is in mmol/min/g catalyst

Table 8.11 Comparison of ethane reactivity of $NbPMo_{12}pyr$ for different flow compositions at 380°C, 0 psig, on low pressure reactor, using 0.6 mL of catalyst.

Flowrates	Conversion		Selectivity			STY[a]	
(mL/min)	C_2	O_2	CO_x	$C_2^=$	Acetic	$C_2^=$	Acetic
16: 8: 16: 20	15.3	47.7	57.1	39.1	3.8	0.050	0.005
15: 5: 15: 20	6.4	36.8	39.1	53.6	7.3	0.037	0.005
16: 4: 16: 20	12.9	77.2	50.1	44.3	5.6	0.062	0.008

[a]STY is in mmol/min/g catalyst

Table 8.12 Comparison of ethane reactivity of various metal-exchanged *M*PMo_{12}pyr at 380°C, 0 psig, 16: 8: 16: 20 mL/hr (ethane: oxygen: helium: steam) on low pressure reactor.

Catalyst	Conversion		Selectivity			STY[a]	
	C_2	O_2	CO_x	$C_2^=$	Acetic	$C_2^=$	Acetic
$TaPMo_{12}$pyr	0.1	0.4	87.6	8.8	3.6	$1.1x10^{-4}$	$1.6x10^{-5}$
$SbPMo_{11}V$pyr	0.6	1.0	10.7	86.1	3.2	0.012	$4.5x10^{-4}$
$ZrPMo_{12}$pyr	0.2	0.6	34.8	63.3	1.9	0.001	$3.8x10^{-5}$
$TiPMo_{12}$pyr	1.3	6.0	81.4	18.0	0.6	0.006	$1.9x10^{-4}$
$NbPMo_{12}$pyr	15.3	47.7	57.1	39.1	3.8	0.050	0.005

[a]STY is in mmol/min/g catalyst

Table 8.13 Ethylene reactivity of $NbPMo_{12}pyr$ at 0 psig, 16: 8: 16: 20 mL/hr (ethylene: oxygen: helium: steam) on low pressure reactor.

T	Conversion			Selectivity[a]					STY[b]
(C)	$C_2^=$	O_2	CO_x	Acetic	AcAld	EtOH	MeAc	EtAc	Acetic
380	28.0	100	76.7	17.0	0.58	0.04	0.02	0.03	0.042
340	27.3	98.2	68.9	23.1	0.60	0.09	0.13	0.20	0.054
280	13.8	48.7	65.4	24.7	0.54	0.46	0.74	0.75	0.030
240[c]	1.8	8.6	64.5	30.4	1.1	2.5	0.31	1.1	0.006
240[d]	1.7	8.8	71.9	25.9	0.36	1.4	0.03	0.36	0.005

[a]AcAld = acetaldehyde, EtOH = ethanol, MeAc = methyl acetate, EtAc = ethyl acetate

[b]STY is in mmol/min/g catalyst

[c]Using D_2O was source of steam

[d]One hour after removal of D_2O from gas stream. Data is from the average of the second hour.

CHAPTER NINE

SUMMARY AND CONCLUSIONS FOR PART TWO

Previous work[1,2] showed that the niobium- and pyridine-exchanged HPA materials were active and selective in the oxidation of light alkanes, specifically *n*-butane and propane, to liquid oxygenates, maleic acid and acrylic acid, respectively. Production of maleic acid from *n*-butane was as high as 0.84 mmol/min/g catalyst at 380°C and flow rates of 32: 16: 32: 40 mL/min of *n*-butane: oxygen: helium: steam, using $NbPMo_{12}$pyr. The incorporation of vanadium into the HPA precursor was important to have an active catalyst for the conversion of propane to acrylic acid (as high as 0.62 mmol/min/g catalyst at 380°C and 32: 16: 32: 40 mL/min of propane: oxygen: helium: steam). In this work, the application of these catalysts to ethane oxidation to acetic acid and ethylene was explored, studying a variety of reaction parameters, e.g., reaction temperature and pressure, reactant feed composition, and catalysts composition.

Increased amounts of steam (0 to 10 mL/min) at elevated pressure (230 psig) increased the selectivity of $NbPMo_{12}$pyr to both ethylene and acetic acid, but lowered conversion. At 230 psig and 280°C, ethane conversion decreased from 15.0% without steam to 6.0% with 10 mL/min of steam. At these conditions, CO_x selectivity decreased from 83.4 to 64.5% as steam was increased. Acetic acid selectivities increased from 3.9% without steam to 12.4% with 10 mL/min of steam. No improvement in acetic acid STY could be obtained simply by varying steam flow rates (STY was 0.002 to 0.003 mmol/min/g catalyst over the steam range of 0 to 10 mL/min). At this pressure, increasing temperatures (from 240 to 300°C) increased ethane conversion from 0.4 to 8.1%, but also increased selectivity to CO_x (from 18.3% to 59.5%). The temperature increase decreased acetic acid selectivity from 22.6% to 4.8%. Lower GHSV at elevated

pressure (230 psig, 280°C) caused the ethylene and acetic acid to over-oxidize to CO_x (up to 83% selectivity). A decrease in acetic acid production, from 0.003 to $4.9x10^{-4}$ mmol/min/g catalyst was observed as space velocity decreased from 4500 to 1200 hr^{-1}.

Increased amounts of steam (0 to 20 mL/min) also increased the selectivity of $NbPMo_{12}$pyr to both ethylene and acetic acid at atmospheric pressure while lowering conversion. Ethane conversion was 30.5% without steam and decreased to 18.1% with 20 mL/min of steam. CO_x selectivity decreased from 65.1 to 38.1% while acetic acid increased from 0.6 to 14.0% for the same conditions, respectively. The maximum STY of acetic acid obtained with $NbPMo_{12}$pyr obtained was 0.021 mmol/min/g catalyst at 380°C, 0 psig, and flows of 16: 8: 16: 20 mL/min of ethane: oxygen: helium: steam (on the high pressure reactor). The selectivity to ethylene and acetic acid improved at lower temperatures (as low as 300°C), but ethane conversion decreased. The overall STY of the products (ethylene and acetic acid) was best at 380°C.

The incorporation of vanadium into the Keggin unit on acetic acid production was examined at 230 psig and 280°C on the high pressure reactor. The conversion for $NbPMo_{11}$Vpyr (2.2%) was less than that obtained under the same conditions (on the same reactor) for $NbPMo_{12}$pyr (6.0%). No change was observed in acetic acid selectivity (13.0% for $NbPMo_{11}$Vpyr and 12.4% for $NbPMo_{12}$pyr). STY of ethylene was higher for $NbPMo_{11}$Vpyr at 0.008 mmol/min/g catalyst (0.006 mmol/min/g catalyst for $NbPMo_{12}$pyr). STY of acetic acid was slightly lower for $NbPMo_{11}$Vpyr at 0.002 mmol/min/g catalyst (0.003 mmol/min/g catalyst for $NbPMo_{12}$pyr). At elevated pressure (230 psig) the addition of vanadium into the Keggin precursor primarily improved selectivity to ethylene, but did not affect the formation of acetic acid.

The effect of vanadium was also examined at atmospheric pressure and 380°C on the *high* pressure reactor. The conversion for $NbPMo_{11}Vpyr$ (15.5%) was again less than that obtained under the same conditions (on the same reactor) for $NbPMo_{12}pyr$ (18.1%). $NbPMo_{12}pyr$, however, had only 14.0% selectivity to acetic acid. $NbPMo_{11}Vpyr$ had 31.0% selectivity to acetic acid at atmospheric pressure, resulting in an increased STY of 0.062 mmol/min/g catalyst ($NbPMo_{12}pyr$ had 0.021 mmol/min/g catalyst of acetic acid). The addition of vanadium into the Keggin precursor had a favorable affect on the acetic acid formation at atmospheric pressure.

Proper analysis of some of the data could not be done due to inconsistencies between the two different reactors used. Although ethane conversions were only slightly lower for $NbPMo_{12}pyr$ between the two reactors (18.1 and 15.3% conversion on the high and low pressure system, respectively), more CO_x was observed in the low pressure reactor (57.1% vs. 38.1% for $NbPMo_{12}pyr$ at 380°C, 0 psig, and 16: 8: 16: 20 mL/min ethane: oxygen: helium: steam) than on the high pressure reactor. This resulted in lower ethylene selectivity and an order of magnitude lower acetic acid selectivity on the low pressure reactor. The low pressure reactor measured only 0.005 mmol/min/g catalyst, instead of the 0.021 mmol/min/g catalyst found by the high pressure reactor for $NbPMo_{12}pyr$ at 380°C, 0 psig, and 16: 8: 16: 20 mL/min ethane: oxygen: helium: steam.

Similar discrepancies between the two reactors were observed for $NbPMo_{11}Vpyr$, although the conversion difference was greater (9.4% on the low pressure reactor vs. 15.5% on the high pressure reactor). More CO_x was observed on the low pressure reactor (46.0% vs. 32.7% for $NbPMo_{11}Vpyr$ at 380°C, 0 psig, and 16: 8: 16: 20 mL/min ethane: oxygen: helium: steam) than on the high pressure reactor. Acetic acid selectivity (5.0%)

was significantly lower on the low pressure reactor than on the high pressure reactor (31.0%). The decrease in acetic acid selectivity was reflected in the lower STY of acetic acid on the low pressure reactor, 0.006 mmol/min/g catalyst, instead of 0.062 mmol/min/g catalyst. The deactivation effect due to reactor configurational differences appeared to be more pronounced for $NbPMo_{11}V$pyr than $NbPMo_{12}$pyr.

The addition of both Nb and pyridine with the HPA was crucial for active catalyst formation, for reactions both at atmospheric pressure and 230 psig. The acid forms, PMo_{12} and $PMo_{11}V$, had no activity for ethane oxidation, either at atmospheric pressure or 230 psig. The exchange of Nb alone to make $NbPMo_{12}$ and $NbPMo_{11}V$ did not improve the activity. Only the incorporation of both Nb and pyridine resulted in an active catalyst for both the PMo_{12} and $PMo_{11}V$ systems. Substitution of other metals for Nb (Ta, Sb, Ti, and Zr) did not achieve significant ethane conversion.

Variations in the Nb/Keggin loading for $NbPMo_{12}$pyr and $NbPMo_{11}V$pyr were studied on the low pressure reactor system. $NbPMo_{12}$pyr had a maximum acetic acid production (on the low pressure reactor) of 0.007 mmol/min/g catalyst for a Nb/Keggin loading of 0.8 and 1.0, at atmospheric pressure. The STY of ethylene also increased as a function of Nb loading, up to a maximum of 0.092 mmol/min/g catalyst at a loading of 0.8. $NbPMo_{11}V$pyr had maximum acetic acid production at atmospheric pressure (on the low pressure reactor) with the Nb/Keggin loading of 0.87, at 0.009 mmol/min/g catalyst. Ethylene STY at this loading was also at maximum (0.086 mmol/min/g catalyst). The $NbPMo_{11}V$pyr catalyst at Nb/Keggin of 0.68 (Holles material) gave significantly more acetic acid STY on the high pressure reactor vs. the low pressure reactor (0.061 vs. 0.006 mmol/min/g catalyst). This appeared to not be the optimal Nb loading, and it would be

beneficial to repeat the reaction at atmospheric pressure on a properly configured reactor for 0.87 Nb/Keggin to determine whether the maximum STY of acetic acid is greater than 0.061 mmol/min/g catalyst.

Sources of raw material for catalyst preparation affected the activity of the catalyst. $NbPMo_{11}Vpyr$ prepared by Holles from synthetic Keggin ($PMo_{11}V$) and $NbCl_5$ at a Nb/Keggin loading of 0.68 had only 9.4% conversion (on the low pressure reactor, at 380°C, 0 psig, and 16: 8: 16: 20 mL/min ethane: oxygen: helium: steam). This same catalyst showed 15.5% conversion at the same reaction conditions on the high pressure reactor. $NbPMo_{11}Vpyr$ prepared at the same Nb/Keggin loading (0.68) using $PMo_{11}V$ obtained from Pred Materials and ammonium niobium oxalate had 15.7% conversion (compared to 9.4% for the Holles material on the same reactor under the same conditions) on the low pressure reactor. Selectivities were similar for both materials (46% CO_x, 50% ethylene, and 4% acetic acid). Because the Holles material had higher conversion and acetic acid STY (0.061 mmol/min/g catalyst) on the high pressure reactor, it is likely that the $NbPMo_{11}Vpyr$ made from commercial Keggin and ammonium niobium oxalate will perform even better on the high pressure reactor configuration and have even higher yield of acetic acid.

The results of this work suggest areas of further study, after proper feed configuration is achieved on the low pressure reactor system. Specifically, comparisons for both $NbPMo_{12}pyr$ and $NbPMo_{11}Vpyr$ activity at 280°C should be made between new runs at atmospheric pressure and the previous work at 230 psig to determine whether the atmospheric reactions have improved selectivity to acetic acid. $NbPMo_{12}pyr$ showed higher ethane conversion at higher pressures (from 2.0% to 6.0%) but similar acetic acid

selectivity (13.5% and 12.4%) on the low and high pressure reactor, respectively, for atmospheric and 230 psig reactions, respectively. Because the low pressure reactor appeared to have lower acetic acid production even for identical conditions and catalysts, atmospheric pressure reactions could in fact have even higher acetic acid selectivity on a properly configured reactor.

The difference between $NbPMo_{12}$pyr and $NbPMo_{11}$Vpyr at atmospheric pressure at 380^{o}C was not significant for data measured under the same conditions on the low pressure reactor. The low pressure reactor measured 0.004 vs. 0.006 mmol/min/g catalyst of acetic acid for $NbPMo_{12}$pyr and $NbPMo_{11}$pyr, respectively, while the high pressure reactor reported 0.021 and 0.062 mmol/min/g catalyst of acetic acid for $NbPMo_{12}$pyr and $NbPMo_{11}$pyr, respectively, for the same conditions. This could again be due to reactor configurational issues and needs to be addressed further.

Configurational differences between the low and high pressure reactor may also have reduced some of the effect on acetic acid formation due to Nb/ Keggin loading in $NbPMo_{12}$pyr and $NbPMo_{11}$Vpyr. Maximum STY of ethylene and acetic acid was observed at Nb/Keggin of 0.8 for $NbPMo_{12}$pyr at atmospheric pressure and 380^{o}C (0.092 and 0.007 mmol/min/g catalyst, respectively). Maximum STY of ethylene and acetic acid was observed at Nb/Keggin of 0.87 for $NbPMo_{11}$Vpyr at atmospheric pressure and 380^{o}C (0.086 and 0.009 mmol/min/g catalyst, respectively). Variations in Nb/Keggin loadings were done using $NbPMo_{11}$Vpyr prepared by Holles and co-workers on the low pressure reactor. $NbPMo_{11}$Vpyr prepared using PMo_{11}V obtained from Pred Materials and ammonium niobium oxalate had higher ethane conversion (15.7% compared to 9.4% for the Holles material) on the same reactor under the same conditions. Further study of

the effect of Nb loadings in both $NbPMo_{12}$pyr and $NbPMo_{11}V$pyr (using the $PMo_{11}V$ from Pred Materials and ammonium niobium oxalate) on a properly configured reactor system would be of interest.

Higher ethane/oxygen ratios appeared to increase the selectivity to acetic acid. At a ratio of 4:1, the ethane conversion was 12.9% for $NbPMo_{12}$pyr at atmospheric pressure, compared to 15.3% at a ratio of 2:1, while selectivity to acetic acid increased to 5.6% from 3.8%. The acetic acid STY increased to 0.008 mmol/min/g catalyst for a ratio of 4:1 (compared to 0.005 for 2:1 ethane/oxygen ratio), suggesting that it may be possible to continue to increase acetic acid production by increasing the ethane/oxygen ratio even further (10:1 and greater). Similar variations in ethane/oxygen ratios should also be done with the $NbPMo_{11}V$pyr.

Feeding ethylene in the place of ethane resulted in the formation of acetic acid. At low conversions, selectivity to methyl acetate, ethyl acetate, and ethanol increased, suggesting that the acetic acid may be formed from an adsorbed ethoxy group on the catalyst surface. Steam from the feed is involved in the formation of acetic acid. Deuterated acetic acid was observed in the product when D_2O was used to provide steam to the reaction. It would be interesting to continue mechanistic studies after low pressure reactor modification to determine the true primary products of reaction. The formation of other deuterated products using D_2O to provide steam, such as methyl acetate, ethyl acetate and ethanol should be closely monitored at low ethylene conversions to determine which species are important in ethylene conversion to acetic acid. Ethylene reactions should also be performed using a ^{13}C-labelled solution of each of these compounds as the

water feed to determine whether the ^{13}C label appears in acetic acid. This would provide evidence for what surface species are involved in acetic acid formation.

(1) Davis, M. E. *et al., Angew. Chem., Int. Ed.* **2002**, *41*, 858.

(2) Holles, J. H. *et al., J. Catal.* **2003**, *218*, 42.

CHAPTER TEN

CONCLUSIONS

This thesis was composed of two separate and unrelated projects. The first project examined the preparation of base-containing molecular sieves for strong base catalysis, e.g., the Michael addition reaction. The objective of this project was to incorporate a covalently attached moiety (e.g., an ammonium or phosphonium functionality) into the pore space of zeolite *BEA to allow the incorporation of a strong base, OH^-, within a molecular sieve. An ammonium functional group could not be used in OFMS preparation because it exhibited degradation after heating to 100^oC. It was not expected that the organic group in Q-*BEA would survive either the zeolite synthesis (at 140^oC) or the SDA extraction. Further work was done to attempt to incorporate a phosphonium functionality into an OFMS.

The phosphonium functionality was prepared by nucleophilic displacement of a halogen-containing alkyl group with trimethylphosphine. Bromopropyl-functionalized mesoporous silica, Br-CPG, was reacted to create the phosphonium functionality at a yield of 86%. This resulted in an organic loading of approximately 0.36 mmol/g of phosphonium on CPG. Heat treatment of the phosphonium-containing CPG showed the bromide form was stable to 300^oC under vacuum. Similar reactions were done with bromopropyl-functionalized *BEA. The *BEA structure was stable to both extraction and nucleophilic displacement reactions. Only 21% of the bromopropyl-functional groups were reacted, resulting in an organic loading of 0.0084 mmol/g of phosphonium. Lack of reaction of the Br-*BEA material with triphenylphosphine (too large to enter the pores) suggested that the functional groups in the OFMS sample were located within the zeolite pore space. Attempts were made to increase the phosphonium loading in OFMS

materials by using the prepared phosphonium organosilane directly in the zeolite synthesis, but the phosphonium moiety was not stable to any extraction procedure attempted to remove the SDA.

The phosphonium halide-containing samples were ion-exchanged to nitrate using 1 N HNO_3. Titration of the filtrate for removed halides determined that the exchange efficiency of Br^- to NO_3^- was 56% for the P^+Br^--CPG material. No removed halides could be detected in the P^+Br^--*BEA samples, however. Shape-selective ion-exchange with $NaBPh_4$, which was too large to enter the *BEA pores, also suggested that the phosphonium moieties were located within the zeolite pores. Finally, ion-exchange to the hydroxide form of the materials had a 72% exchange efficiency from NO_3^- to OH^- for the P^+ NO_3^--CPG material, giving an overall exchange efficiency of 40% from bromide to hydroxide. Exchange results for the P^+ NO_3^--*BEA did show removal of nitrate (0.008 mmol/g), but this was similar to the control Si-*BEA sample and was not conclusive.

Neither the ion-exchange tests described nor the catalytic experiments were able to prove the presence of a phosphonium hydroxide moiety within an OFMS. All of the uncalcined *BEA samples were capable to catalyzing the Knoevenagel condensation reaction of benzaldehyde and malononitrile, even extracted Si-*BEA. Michael addition reactions with methylvinylketone did suggest the existence of a base site within P^+OH^--CPG that was not due to physisorbed hydroxide. No significant reactivity was observed for the Michael addition in any of the *BEA samples tested. Residual TEAF from extraction, physisorbed hydroxide from the ion-exchange, and the low number density of the phosphonium groups prevented clear conclusions of the nature of the functional group in the OFMS samples.

Results from the functionalized CPG work show that the process of creating phosphonium-containing materials from a halogen-containing material and subsequent ion-exchange of the halide form to hydroxide to create a heterogeneous material for strong base catalysis is feasible. However, the phosphonium group is susceptible to degradation in chemical environments, suggesting that the incorporation of a quaternary moiety (ammonium or phosphonium) within a porous material is only appropriate where temperature and environment are mild.

The second part of this thesis examines the use of niobium- and pyridine-exchanged heteropolyanions as catalyst precursors for the selective oxidation of light alkanes with dioxygen. $NbPMo_{12}$pyr showed higher ethane conversion at higher pressures (from 2.0% to 6.0%) but similar acetic acid selectivity (13.5% and 12.4%) at 280^{o}C for atmospheric and 230 psig reactions, respectively. No improvement in acetic acid STY could be obtained simply by varying steam flow rates or changing reaction temperatures while keeping all other parameters constant. Lower GHSV caused the ethylene and acetic acid to over-oxidize to CO_x. The maximum STY of acetic acid obtained with $NbPMo_{12}$pyr obtained was 0.021 mmol/min/g catalyst at 380^{o}C, 0 psig, and flows of 16: 8: 16: 20 mL/min of ethane: oxygen: helium: steam (on the high pressure reactor).

At elevated pressure (230 psig) the addition of vanadium into the Keggin precursor primarily improved selectivity to ethylene, but did not affect the formation of acetic acid. At atmospheric pressure the addition of vanadium into the Keggin precursor had a favorable affect on the acetic acid formation. The ethane conversion increased slightly, from 1.1 to 2.2% as the pressure was increased from 0 to 230 psig at 280^{o}C.

Ethylene and acetic acid selectivity both decreased with increased pressure. The STY of ethylene and acetic acid were slightly higher under pressure, at 0.008 and 0.002 mmol/min/g catalyst, respectively, because of higher conversion. $NbPMo_{11}Vpyr$ had maximum production of acetic acid at 380°C, 0 psig, and flows of 16: 8: 16: 20 mL/min of ethane: oxygen: helium: steam (on the high pressure reactor), resulting in an increased STY of acetic acid at 0.062 mmol/min/g catalyst. This was the highest STY of acetic acid observed during all of the ethane oxidation experiments.

Proper analysis of some of the data could not be done due to inconsistencies between the two different reactors used. Ethane conversions were only slightly lower for $NbPMo_{12}pyr$ between the two reactors, and more CO_x was observed in the low pressure reactor. This resulted in lower ethylene selectivity and an order of magnitude lower acetic acid selectivity on the low pressure reactor. The conversion difference between the two reactors was greater for $NbPMo_{11}Vpyr$. The deactivation effect due to reactor configurational differences appeared to be more pronounced for $NbPMo_{11}Vpyr$ than $NbPMo_{12}pyr$. Sources of raw material (i.e., $PMo_{11}V$ and niobium source) for catalyst preparation affected the activity of the catalyst. $NbPMo_{11}Vpyr$ prepared using $PMo_{11}V$ obtained from Pred Materials and ammonium niobium oxalate had higher ethane conversion than $NbPMo_{11}Vpyr$ prepared by Holles from synthetic Keggin ($PMo_{11}V$) and $NbCl_5$.

The addition of both Nb and pyridine with the HPA was crucial for active catalyst formation, for reactions both at atmospheric pressure and 230 psig. Substitution of other metals for Nb (Ta, Sb, Ti, and Zr) did not achieve significant ethane conversion. $NbPMo_{12}pyr$ had a maximum ethylene and acetic acid production (on the low pressure

reactor) of 0.092 and 0.007 mmol/min/g catalyst, respectively, for a Nb/Keggin loading of 0.8, at atmospheric pressure. $NbPMo_{11}Vpyr$ had maximum ethylene and acetic acid production (also on the low pressure reactor) of 0.086 and 0.009 mmol/min/g catalyst, respectively, for a Nb/Keggin loading of 0.87, at atmospheric pressure. Since the high pressure reactor configuration gave better acetic acid production at atmospheric pressure with $Nb_{0.4}PMo_{12}pyr$ and $Nb_{0.68}PMo_{11}Vpyr$, the optimal Nb/Keggin loadings of $Nb_{0.8}PMo_{12}pyr$ and $Nb_{0.87}PMo_{11}Vpyr$ should be re-examined.

Higher ethane/oxygen ratios appeared to increase the selectivity to acetic acid for $NbPMo_{12}pyr$ at atmospheric pressure. Similar variations in ethane/oxygen ratios should also be done with the $NbPMo_{11}Vpyr$. Feeding ethylene in the place of ethane resulted in the increased production of acetic acid. Steam from the feed is involved in the formation of acetic acid. Deuterated acetic acid was observed in the product when D_2O was used to provide steam to the reaction. Further mechanistic studies after low pressure reactor modification should be done to determine the true primary products of reaction.

APPENDICES

Appendix A: BTRS, Jr. Reactors

Figure A.1 Autoclave Engineers BTRS, Jr. reactor (high pressure reactor).

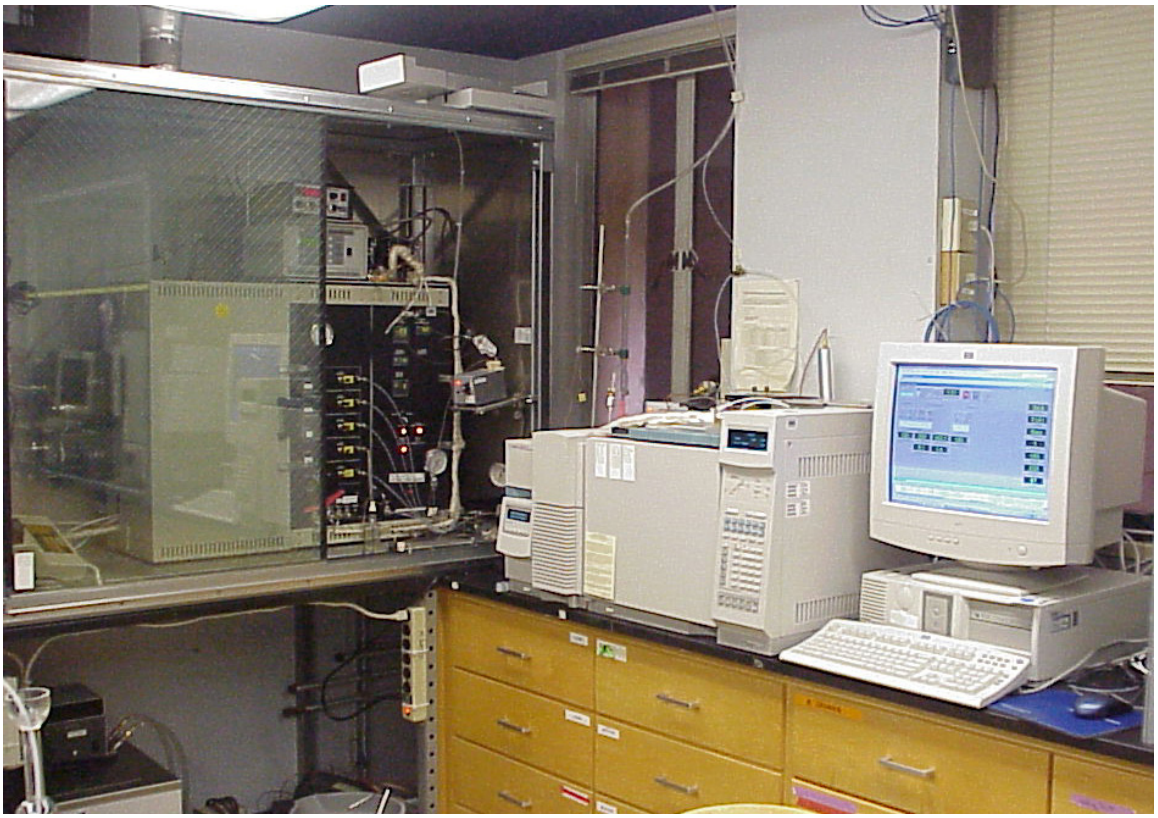

Figure A.2 Autoclave Engineers BTRS, Jr. reactor (low pressure reactor).

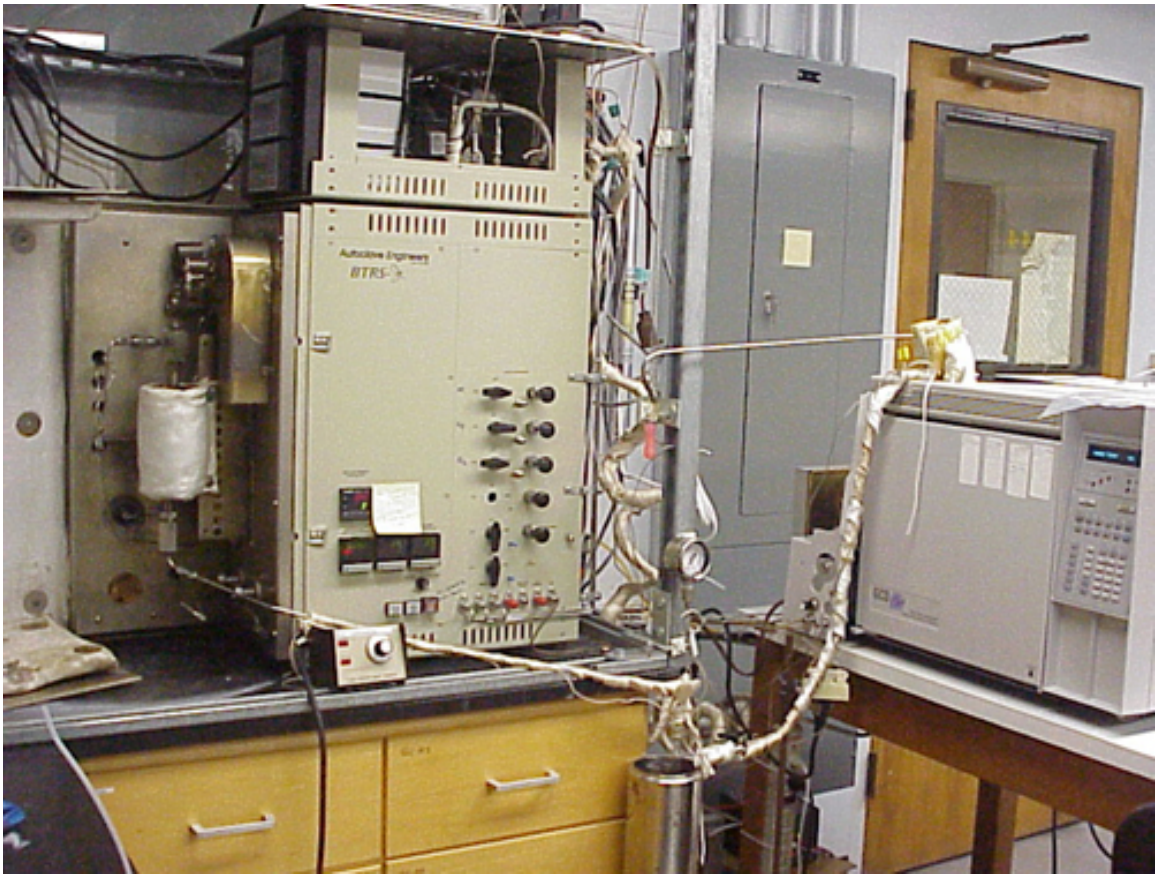

Figure A.3 Configuration of reactor tube in the reactor furnace on high pressure reactor.

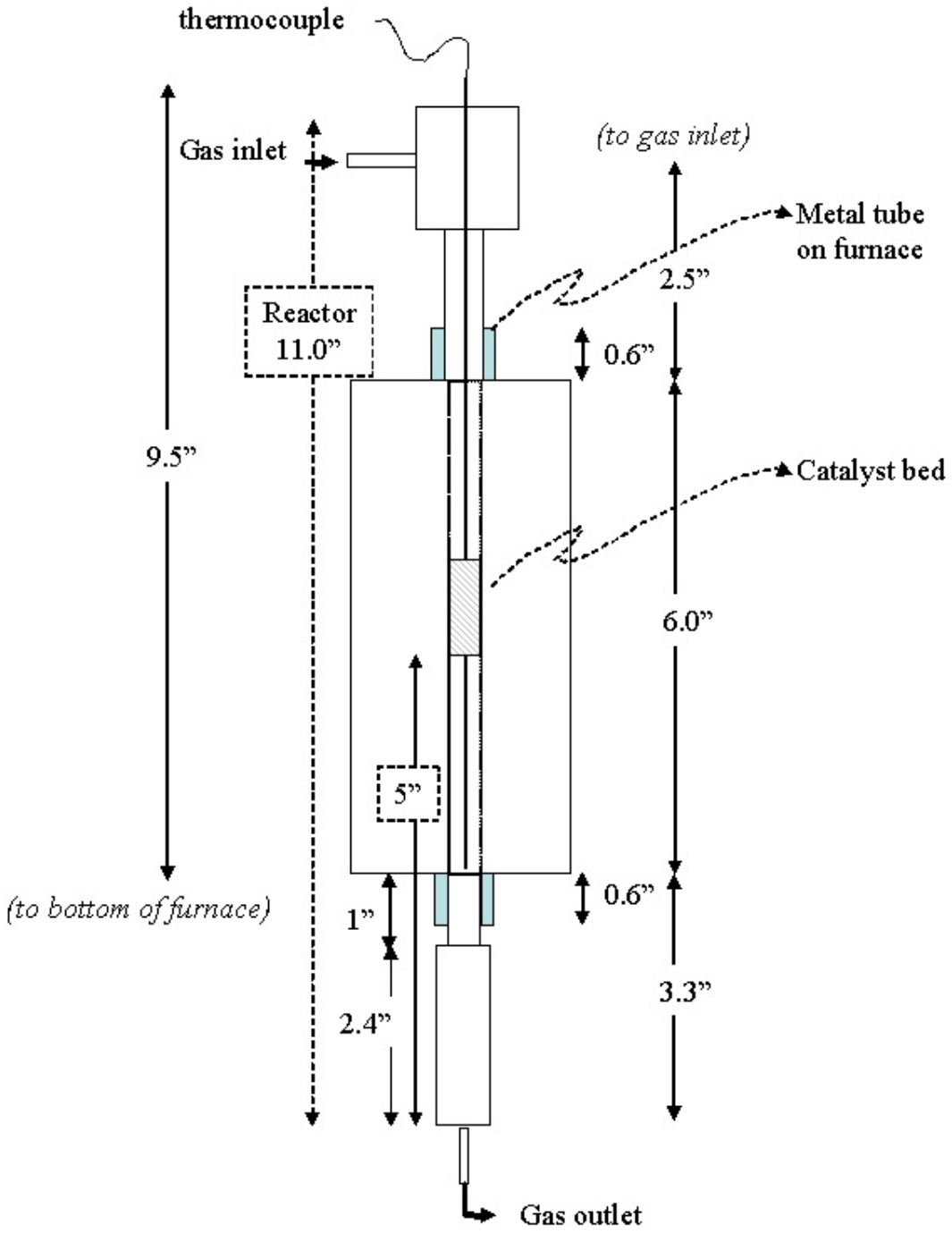

Figure A.4 Configuration of reactor tube in the reactor furnace on low pressure reactor.

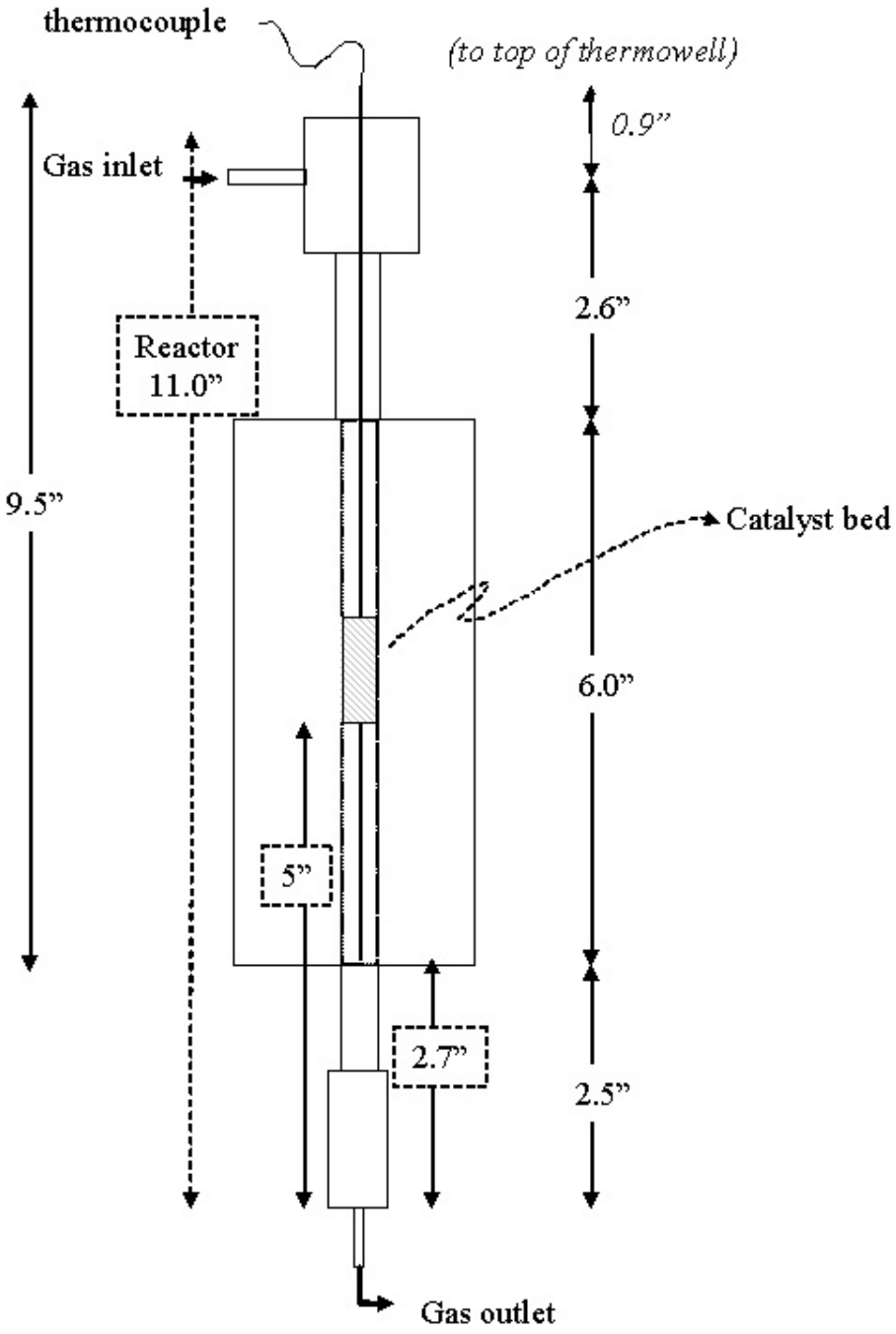

Figure A.5 Temperature profile in reactor tube filled with glass wool on low pressure reactor. (● - temperature profile when temperature controller is set to 380°C).

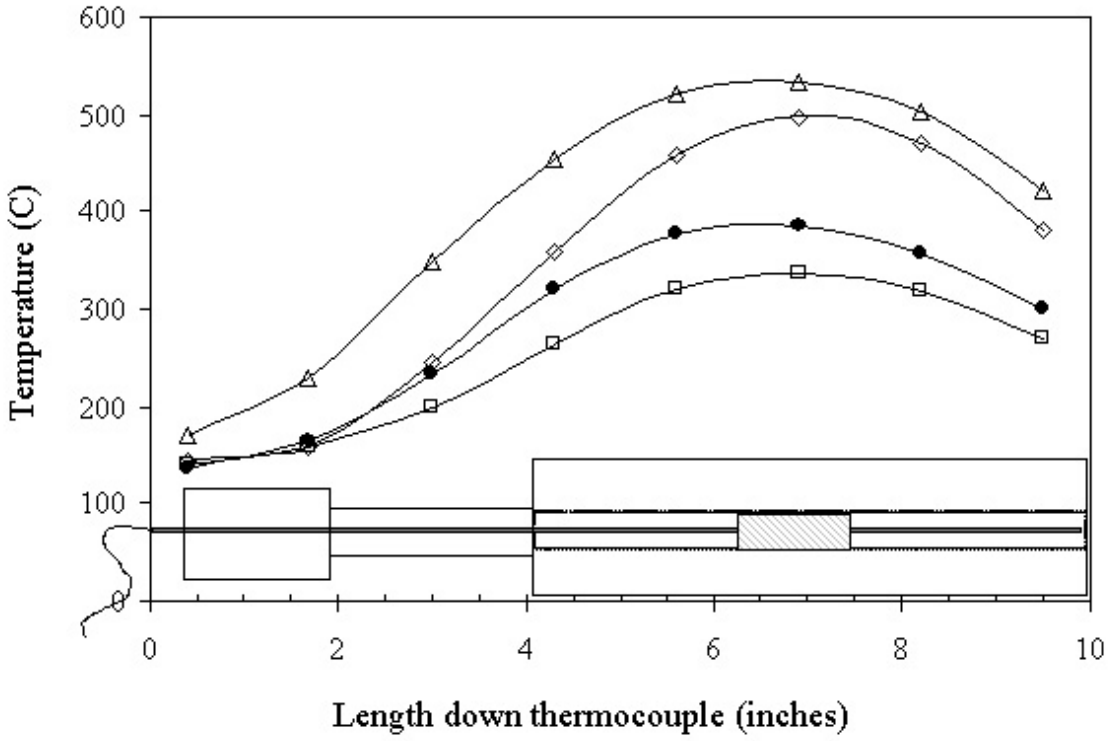

Appendix B: Flammability Calculations

Flammability calculations were performed to ensure that the ethane/oxygen mixtures used as feed for the reaction studies were non-flammable. The author would like to acknowledge Marcia Cooper and Professor Joseph Shepherd for their assistance in providing the data and methods for the calculations.

B.1 Flammability Limit Data

Data for the flammability range for a variety of gases may be found in Bulletin 627 from the Bureau of Mines.[1] The data are presented in the form of charts and graphs, at particular temperatures and pressures (usually room temperature and atmospheric pressure) and levels of inert (data gathered in air, oxygen, or with additional inert). The flammability range consists of a lower flammability limit (LFL) and upper flammability limit (UFL). The limits are *usually* expressed in terms of volume percent of the hydrocarbon in the gas mixture. Below the LFL, the gas stream cannot sustain a flame. Likewise, above the UFL, no flame may be maintained. It is between the two limits that the mixture is flammable, either by encountering an ignition source or by self-igniting if above the auto-ignition temperature (AIT). Other relevant information, such as the AIT, heat of combustion (ΔH_c), and quenching distances for a traveling flame front, may also be found in the Bulletin.

B.2 Temperature Corrections

Because the flammability ranges usually presented in the data are at room temperature, a correction must be applied to adjust the range for elevated temperatures, such as the reaction temperatures in this study. The LFL and UFL are affected by temperature, where the LFL is decreased and the UFL is increased, thereby *widening* the

flammability range with elevated temperature. The limits change linearly with temperature for a particular hydrocarbon:[1]

$$LFL_{T(C)} = LFL_{25\,C} - (0.75 / \Delta H_c) \cdot (T - 25)$$

$$UFL_{T(C)} = UFL_{25\,C} + (0.75 / \Delta H_c) \cdot (T - 25)$$

where

$LFL_{T(C)}$ is the lower flammability limit at temperature T (in ^oC)

$LFL_{25\,C}$ is the lower flammability limit at room temperature (25^oC)

ΔH_c is the heat of combustion of the hydrocarbon in kcal/mol at 25^oC

$UFL_{T(C)}$ is the upper flammability limit at temperature T (in ^oC)

$UFL_{25\,C}$ is the upper flammability limit at room temperature ($25\ ^oC$)

Charts developed from experimental data are also available in Bulletin 627 that provide this empirical correlation for hydrocarbons. (Note the ΔH_c of ethane is 341.3 kcal/mol, taken from Table 2 of the Bulletin, page 21.)

B.3 Pressure Corrections

Increase in pressure above atmospheric pressure also affects the LFL and UFL. The effect is more significant in the UFL. No empirical equations for flammability limits as a function of pressure were found in the author's search for flammability data (although such correlations may exist). Charts developed from experimental data at a variety of pressures for some gases are presented in the Bulletin, although the information available is limited. In particular, Figure 38 from Bulletin 627 was used for the ethane flammability calculations as a function of pressure (in air, at 25^oC) for the reactivity experiments conducted in this study. The chart presents the flammability limits as a

function of added inert (nitrogen) beyond what would be found in air at several pressures (see Figure B.1). The amount of oxygen in the reaction stream was used to calculate what would be an equivalent amount of "air," using the amount of helium *and* steam fed to substitute as nitrogen. (Note that different inert gases suppress flammability differently, and it is an approximation to the calculations by assuming that the helium and steam behave the same as nitrogen. This was necessary because no information was available for the behavior of ethane under pressure with oxygen and added helium.) The percentage of excess inert added was then calculated and used to read the LFL and UFL at 0 psig for atmospheric reactions and 250 psig for the pressure reactions (an approximation for 230 psig, which was the actual reaction pressure) from Figure B.1. The LFL and UFL at reaction pressure were then adjusted for temperature as described above and used to determine if the proposed reactant gas stream was flammable.

B.4 Quenching Distance

Although the ethane reactions were run using non-flammable reactant mixtures, the quenching distance of ethane was researched to give further confidence in the safety of the experimental setup. A traveling flame front will be extinguished in any diameter smaller than its quenching distance. In typical applications a flame arrestor, which restricts the diameter of flow, is used to prevent the flame front from traveling through a system. Note that the catalyst bed itself will act as a flame arrestor. The quenching distance of ethane is 1.8 mm.[2] The addition of flame arrestors into the BTRS, Jr., reactor assemblies was not necessary, however, because the 1/8-inch diameter tubing used for gas flow has an inner diameter of 1.57 mm, smaller than ethane's quenching distance. The tubing on either side of the reactor tube would not allow any flames to propagate

through the system. Additionally, any sharp increase of pressure in the system would cause the pressure relief disk on the high pressure reactor (set at approximately 1600 psig) to rupture and safely vent the contents of the reactor.

B.5 References

(1) Zabetakis, M. G.; Bureau of Mines, 1965; Vol. Bulletin 627.

(2) Turns, S. R. *An Introduction to Combustion: Concepts and Applications*; McGraw-Hill: New York, 1996.

Figure B.1 Ethane flammability data for various pressures.[1]

Reprinted with permission from US Bureau of Mines.

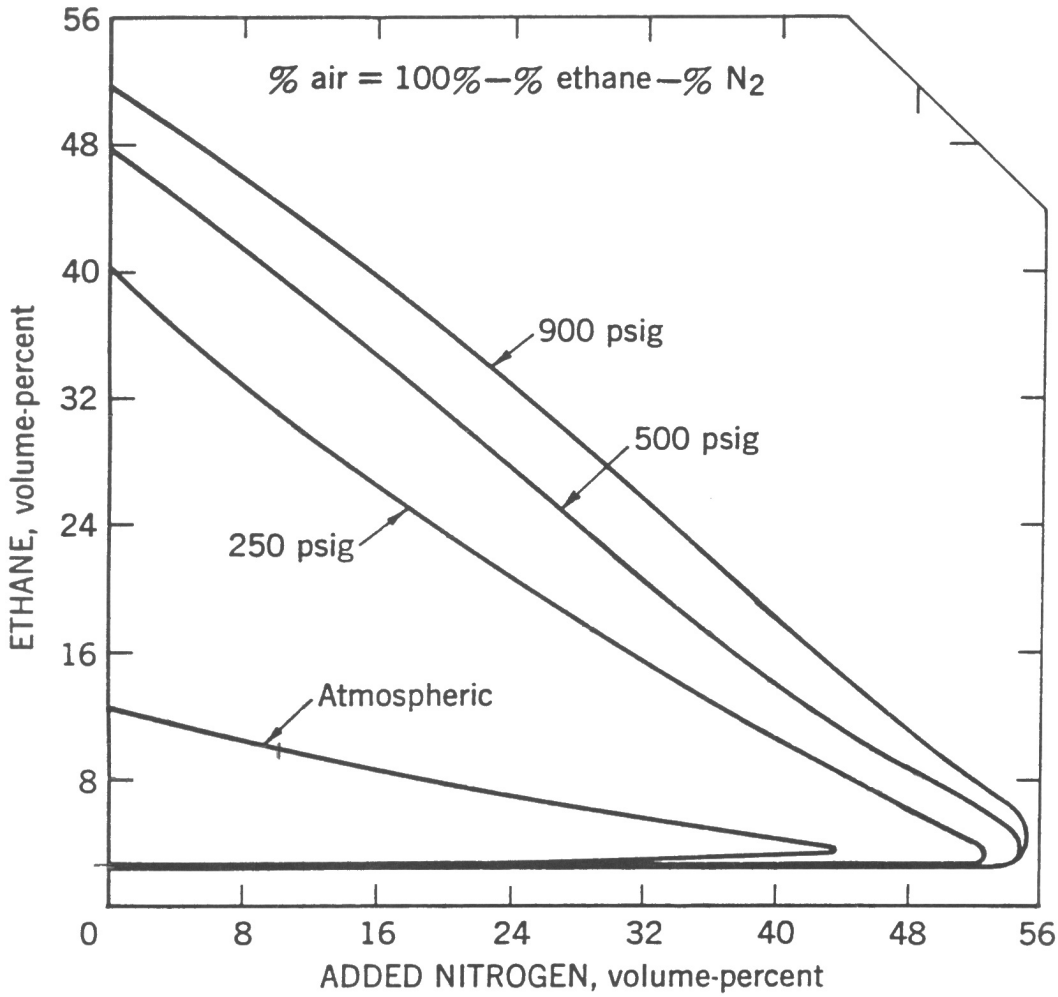

FIGURE 38.—Effect of Pressure on Limits of Flammability of Ethane-Nitrogen-Air Mixtures at 26° C.

Appendix C: Reactivity Data Tables

The following are tables of data used to create the figures of Chapter 8, as indicated in the table captions.

Table C.1 Ethane reactivity of $NbPMo_{12}pyr$ at 280°C, 230 psig, 8: 4: 27: *x* mL/hr (ethane: oxygen: helium: steam) on high pressure reactor.

Data for Figures8.6, 8.7, and 8.8

Steam Feed	Conversion		Selectivity			STY[a]	
(mL/min)	C_2	O_2	CO_x	$C_2^=$	Acetic	$C_2^=$	Acetic
0	15.0	87.4	83.4	12.7	3.9	0.009	0.003
1	14.8	86.2	81.8	14.2	4.0	0.010	0.003
2	13.1	86.8	83.9	12.6	3.6	0.009	0.003
3	11.0	61.6	79.9	16.2	3.9	0.010	0.002
4	7.5	40.4	70.8	23.9	5.3	0.010	0.002
5	8.6	40.9	71.9	22.8	5.3	0.010	0.002
10	6.0	28.4	64.5	23.2	12.4	0.006	0.003

[a]STY is in mmol/min/g catalyst

Table C.2 Ethane reactivity of $NbPMo_{12}pyr$ at 280°C, 230 psig, (8: 4: 27: 10) mL/hr (ethane: oxygen: helium: steam) on high pressure reactor. Volume of catalyst varied.

Data for Figures 8.9 and 8.10

GHSV	Conversion		Selectivity			STY[a]	
(hr^{-1})	C_2	O_2	CO_x	$C_2^=$	Acetic	$C_2^=$	Acetic
1225	9.3	52.8	83.0	13.0	4.0	0.002	4.9x10-4
2138	3.3	12.1	55.6	34.7	9.7	0.003	0.001
4523	6.0	28.4	64.5	23.2	12.4	0.006	0.003

[a]STY is in mmol/min/g catalyst

Table C.3 Ethane reactivity of $NbPMo_{12}pyr$ at 380°C, 0 psig, 16: 8: 16: *x* mL/hr (ethane: oxygen: helium: steam) on high pressure reactor.

Data for Figures 8.11, 8.12, and 8.13

Steam Feed	Conversion			Selectivity		STY[a]	
(mL/min)	C_2	O_2	CO_x	$C_2^=$	Acetic	$C_2^=$	Acetic
0	30.5	99.1	65.1	34.4	0.6	0.099	0.002
2	28.2	88.2	60.6	38.7	0.7	0.108	0.002
10	18.2	50.2	41.8	49.5	8.7	0.100	0.008
20	18.1	46.1	38.1	47.8	14.0	0.072	0.021

[a]STY is in mmol/min/g catalyst

Table C.4 Ethane reactivity with temperature of $NbPMo_{12}pyr$ at 0 psig, 16: 8: 16: 20 mL/hr (ethane: oxygen: helium: steam) on high pressure reactor, except 280°C run on low pressure reactor.

Data for Figure 8.14

Temperature	Conversion		Selectivity			STY[a]	
(C)	C_2	O_2	CO_x	$C_2^=$	Acetic	$C_2^=$	Acetic
380	18.1	46.1	38.1	47.8	14.0	0.072	0.021
340	6.5	14.0	21.7	59.1	19.2	0.037	0.012
300	3.1	6.5	10.6	57.3	32.1	0.017	0.010
280[b]	2.0	6.3	24.8	61.6	13.5	0.006	0.001

[a]STY is in mmol/min/g catalyst

[b]Flows are 8: 4: 25: 10 mL/min, GHSV = 4700 hr^{-1}, run on low pressure reactor.

Table C.5 Ethane reactivity with Nb loading of $NbPMo_{12}pyr$ at 380°C, 0 psig, 16: 8: 16: 20 mL/hr (ethane: oxygen: helium: steam) on low pressure reactor.

Data for Figures 8.15, 8.16, and 8.17

Nb/Keggin	Conversion		Selectivity			STY[a]	
loading	C_2	O_2	CO_x	$C_2^=$	Acetic	$C_2^=$	Acetic
0	0.6	2.8	69.5	30.5	0	0.002	0
0.04	0.9	3.0	37.5	55.5	7.1	0.006	0.001
0.2	7.6	22.4	34.2	61.1	4.6	0.055	0.004
0.4	15.3	47.7	57.1	39.1	3.8	0.050	0.005
0.6	14.0	51.5	54.0	42.6	3.4	0.081	0.006
0.8	13.6	48.2	51.4	45.2	3.4	0.092	0.007
1.0	12.9	44.2	48.2	47.9	3.9	0.084	0.007

[a]STY is in mmol/min/g catalyst

Table C.6 Ethane reactivity with Nb loading of $NbPMo_{11}Vpyr$ at 380°C, 0 psig, 8: 4: 8: 10 mL/hr (ethane: oxygen: helium: steam) on low pressure reactor, $V_{catalyst}$ = 0.3 mL.

Data for Figures 8.18, 8.19, and 8.20

Nb/Keggin	Conversion		Selectivity			STY[a]	
loading	C_2	O_2	CO_x	$C_2^=$	Acetic	$C_2^=$	Acetic
0.04	1.0	3.2	39.4	56.6	4.0	0.009	0.001
0.12	1.3	3.7	44.7	48.6	6.7	0.015	0.002
0.68	9.4	32.6	46.0	49.0	5.0	0.064	0.006
0.87	8.2	26.8	45.1	49.7	5.3	0.086	0.009
0.98	3.9	13.5	44.2	52.7	3.1	0.043	0.003

[a]STY is in mmol/min/g catalyst